NASA CONTRACTOR REPORT

NASA CR-1841

STUDY OF VIBRATIONAL EXCITATION MECHANISMS OF CO_2 AT HIGH TEMPERATURES

by Joseph W. Rich, Ronald G. Rehm, and Charles E. Treanor

Prepared by
CORNELL AERONAUTICAL LABORATORY, INC.
Buffalo, N. Y. 14221
for Ames Research Center

NATIONAL AERONAUTICS AND SPACE ADMINISTRATION • WASHINGTON, D. C. • MAY 1971

1. Report No.	2. Government Accession No.	3. Recipient's Catalog No.
NASA CR-1841		

4. Title and Subtitle	5. Report Date
Study of Vibrational Excitation Mechanisms of CO_2 at High Temperatures	May 1971
	6. Performing Organization Code

7. Author(s)	8. Performing Organization Report No.
Joseph W. Rich, Ronald G. Rehm and Charles E. Treanor	
	10. Work Unit No.

9. Performing Organization Name and Address	11. Contract or Grant No.
Cornell Aeronautical Laboratory, Inc. Buffalo, New York 14221	NAS 2-4185
	13. Type of Report and Period Covered
12. Sponsoring Agency Name and Address	Contractor Report
National Aeronautics & Space Administration Washington, D.C. 20546	14. Sponsoring Agency Code

15. Supplementary Notes

16. Abstract

Major emphasis has been placed on obtaining models for calculating cross sections for the inelastic collision of a structureless particle with a CO_2 molecule. The CO_2 molecule itself is modeled so that the only participating degrees of freedom are the translational modes, and the rotational and vibrational modes of the CO_2 molecule. The analyses reported are semi-classical in nature.

Results of calculations for the vibrational excitation of CO_2 are reported, for both a model which includes anharmonic coupling among the vibrational modes, and for an approximate normal mode model.

Energy transfer from the (01^10), $(00°1)$, and $(10°0)$ CO_2 states in collision with rare gas atoms was studied using the coupled-mode model. Very close coupling between the symmetric stretching and bending modes is predicted during such collisions.

Special features of a multistate calculation of CO_2 vibrational excitation have been compared with a first order perturbation calculation. It is found that for some CO_2 transitions, several coupled states must be retained for an accurate calculation.

The effects of potential anisotropy and participation of the rotational energy mode were also investigated, using the normal mode model. The rotational mode is shown to make a contribution to vibrational excitation over a considerable range of relative translational energies in the collision. The overall magnitude of the probabilities for vibrational excitation and the degree of participation of the rotational mode show marked dependence on the potential anisotropy. Comparisons of coplanar and three dimensional calculations of the CO_2 bending mode collisional excitation show no significant difference in the two calculations over a large temperature range.

17. Key Words (Suggested by Author(s))	18. Distribution Statement
Carbon Dioxide Vibrational Relaxation	UNCLASSIFIED-UNLIMITED

19. Security Classif. (of this report)	20. Security Classif. (of this page)	21. No. of Pages	22. Price*
UNCLASSIFIED	UNCLASSIFIED	60	3.00

*For sale by the National Technical Information Service, Springfield, Virginia 22151

FOREWORD

The authors would like to acknowledge the assistance of Miss Marcia Williams and Mr. John Moselle, who, in addition to programing the calculations contained in this report, have provided many helpful suggestions in the course of the work. This work was supported by the National Aeronautics and Space Administration, Ames Research Center, under Contract NAS 2-4185. The Ames technical monitor was Mr. Robert McKenzie of the Hypersonic Aerodynamics Branch; the Ames contract administrator was Mr. Robert Dolan of the Contract Administration Section.

ABSTRACT

The work presented is a report on theoretical studies of CO_2 vibrational relaxation. Major emphasis has been placed on obtaining models for calculating cross sections for the inelastic collison of a structureless particle with a CO_2 molecule. The CO_2 molecule itself is modeled by assuming adiabaticity of the electronic motion, so that the only participating degrees of freedom are the translational modes, and the rotational and vibrational modes of the CO_2 molecule. The analyses reported are semiclassical in nature. Methods of analysis, such as first order perturbation theory, specifically applicable only at low thermal velocities are avoided.

An empirical approach to the problem of specifying the intermolecular potential is adopted. The intermolecular potential functions chosen have been simple analytical forms, with parameters which can be varied to investigate their influence, or, alternately, matched to available experimental data. Results of calculations for the vibrational excitation of CO_2 are reported, for both a model which includes anharmonic coupling among the vibrational modes, and for an approximate normal mode model.

Using the coupled-mode model, energy transfer from the $(01^{1}0)$, $(00^{\circ}1)$, and $(10^{\circ}0)$ CO_2 states in collision with rare gas atoms was studied. Very close coupling between the symmetric stretching and bending modes is predicted during such collisions. The asymmetric stretch state $(00^{\circ}1)$ is found to be less strongly coupled to the bending mode, lending support to a "two temperature" kinetic model of the vibrational energy modes for CO_2 - rare gas collisions.

Special features of a multistate calculation of CO_2 vibrational excitation have been examined, and comparison made with a first order perturbation calculation. It is found that for some CO_2 transitions, several coupled states must be retained for an accurate calculation, even at quite low collision energies.

Using the normal mode model, the effects of potential anisotropy and participation of the rotational energy mode were investigated. It is found

that the rotational mode can make a contribution to vibrational excitation over a considerable range of relative translational energies in the collision. The degree of participation of the rotational mode is a strong function of the potential anisotropy. Further, the overall magnitude of the probabilities for vibrational excitation show marked dependence on the potential anisotropy. Both coplanar and three dimensional calculations of the CO_2 bending mode collisional excitation were made; there was no significant difference in the two calculations over a large temperature range.

TABLE OF CONTENTS

LIST OF ILLUSTRATIONS

1. INTRODUCTION

Vibrational relaxation in gases is a nonequilibrium process that has received extensive theoretical and experimental study in recent years. Interest has been occasioned by the importance of this process in high temperature gas flows, in many chemical reactions, and, most recently, in molecular gas lasers. The understanding and prediction of vibrational relaxation mechanisms in CO_2, in particular, is necessary both for analysis of the gas dynamic phenomena occurring upon entry into planetary atmospheres and for performance analysis of CO_2 gas lasers.

The work presented in this report is a theoretical study of CO_2 vibrational relaxation. Emphasis has been placed on calculating cross sections for the inelastic collision of a structureless particle with a CO_2 molecule. The CO_2 molecule itself is modeled by assuming adiabaticity of the electronic motion, so that the only degrees of freedom are the translational modes, and the rotational and vibrational modes of the CO_2 molecule. The remaining paragraphs of this introduction outline, in more detail, some of the considerations entering into the present study.

Considerable progress[1-14] has been made in the calculation of cross sections for vibrational energy excitation in nonpolar diatomic molecules, and in prediction of the overall vibrational relaxation times for such species. It has been shown, however, that a major problem in these calculations is the extreme sensitivity of the cross sections to potential details, particularly at low thermal velocities (Ref. 15, pgs. 685-691). In order to predict accurately the absolute magnitude of the cross section for an inelastic event of this type, the inter- and intramolecular potential functions must be known accurately. Little is known, however, of the intermolecular potential function for CO_2, other than what is available from measurements of virial coefficients. Any choice of a potential function must be regarded as postulational. One requires either detailed molecular scattering experiments or elaborate large-scale quantum mechanical potential calculations in order to establish, ab initio, the correct potential. In the absence of such investigations, the present study adopts an empirical approach to the problem of specifying the intermolecular potential.

The intermolecular potential functions chosen have been simple, analytical forms, with parameters which can be varied to investigate their influence, or, alternately, matched to available experimental data.

As general a treatment as possible was desired. In particular, we have attempted to model those features which distinguish CO_2, a linear triatomic, from the more commonly studied diatomic case. Such features include a more marked departure from spherical symmetry, the influence of the vibrational bending modes, and intermode coupling within the molecule. Several theoretical treatments of CO_2 vibrational relaxation are already extant.[16-22*] However, each of them possesses at least one of the following limitations:

1. Restriction to a first order perturbation approximation.[16, 18-21]
2. Neglect of intermode coupling effects within the CO_2 molecule.[17-19]
3. Neglect of molecular rotation effects and potential anisotropy.[17, 20, 22]

The studies presented in this report examine the effect on CO_2 vibrational excitation of the removal of these restrictions. The analyses are semiclassical in nature. It can be noted that, in recent years, completely classical models have been used to calculate numerically both vibrational energy transfer cross sections[6, 11-14] and reactive scattering cross sections[27, 28] in simple molecules. The reactive scattering calculations, in particular, have met with considerable success in interpreting molecular beam reactive scattering experiments. In the present work, however, it was felt desirable to retain a quantum mechanical description of the vibrational modes of CO_2, although translational and rotational motions of the system are described classically. The quantized nature of the vibrational-energy modes of CO_2 is emphasized by the techniques and phenomena of experimental studies. One example is afforded by recent experiments[20, 29] in which a vibrational fluorescence

*In addition to the work of Refs. 16-22, there have been important recent theoretical studies [23-25] of near-resonant vibration-to-vibration and vibration-to-rotation intermolecular energy transfer between CO_2 and certain other molecular species (N_2, H_2O, H_2). These studies are of the processes controlled by long-range multipole molecular interactions, which are dominant in V-V transfer at temperatures below $\sim 1000°K$.[26] Such processes fall outside the scope of the present investigation.

technique is used to study the collisional deactivation of the first excited state of the asymmetric stretching vibration (00°1) of CO_2 in rare-gas diluents. It appears that this deactivation proceeds by means of intramolecular vibration-to-vibration energy transfer during CO_2 rare-gas collisions. It is found that these results can be interpreted only if Fermi resonance and Coriolis mixing of the CO_2 vibrational states is considered. A second example is the analysis of the behavior and performance of CO_2 infrared lasers.[26] Application of theory to such processes makes a quantum mechanical treatment of the vibrational states extremely desirable.

Finally, it should be mentioned that it is desired to apply the theory developed in this study over a wide range of kinetic temperature. Thus methods of analysis specifically applicable only at low thermal velocities, such as first order perturbation theory, are avoided.

The remainder of the report is in three major sections. Section 2 discusses the model adopted and develops the basic equations used in the study. Section 3 presents calculated results for collision-induced energy transfer processes among the various vibrational modes of the CO_2 molecule. The studies of this section emphasize intramolecular vibration-to-vibration (V-V) processes. Section 4 presents calculated results for collisional excitation of a normal mode model of CO_2. The approximations introduced in this analysis make it appropriate for calculation of the rate for direct translation-to-vibration (T-V) thermal excitation of CO_2, and it complements the V-V calculations of Section 3. Molecular rotational effects are included. The concluding Section, 5, gives a final discussion and summary of the results obtained.

2. MODEL AND GOVERNING EQUATIONS

2.1 BASIC ASSUMPTIONS

We consider the collision of the CO_2 molecule with another molecule, which has been assumed to possess no internal energy modes, i.e., to be a structureless, point-mass type particle. The following approximations are also made:

1. Only the nuclear motion of the CO_2 molecule is specifically considered; no electronic excitation is treated.

2. The rotational and translational motion of the CO_2 - M system is treated classically; a quantum mechanical description of the CO_2 vibrational motion is used.

3. Coupling between the rotational and vibrational motions, created by Coriolis and centrifugal forces, is neglected.

4. The intermolecular potential between CO_2 and the collision partner M is taken to the sum of pairwise interactions between M and each of the atomic nuclei in CO_2.

5. The influence of vibrational motion on the rotational and translational motion of the CO_2 - M system is neglected.

Approximation 5 allows the effect of the CO_2 - M collision to be treated by a time-dependent perturbation acting on CO_2 vibration, as will be made explicit below.

2.2 EXTERNAL MOTION

Under the preceding approximations, the "external" translational and rotational motion of the CO_2 - M is decoupled, and is governed by classical equations of motion, which may be solved separately from the rest of the problem. In the standard fashion, the kinetic energy of translation of the center of mass of the entire molecule-particle system can be ignored, using center-of-mass coordinates, since there is no potential affecting the entire system. We therefore consider a system of space-oriented coordinates x, y, z with origin at the center of mass of the molecule.

The position of the incident particle relative to the scattering center can be described in terms of the standard scattering coordinates (R, Θ, Φ) or $\vec{R}$, as indicated in Fig. 1.

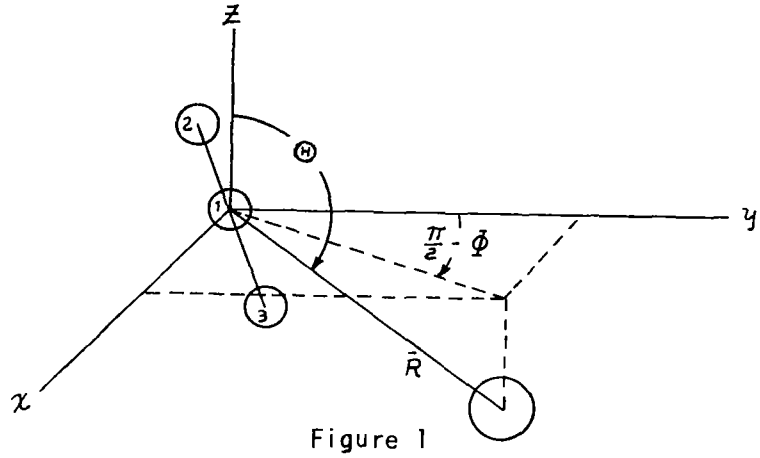

Figure 1

Fig. 2 shows the coordinate system used to describe the rotational motion of the CO_2 molecule. It shows the relationship between a coordinate system (x' y' z') fixed in the molecule and the previously introduced xyz system of Fig. 1. As shown in the figure, the z' axis is the molecular axis, i.e., the line of nuclear centers in the equilibrium configuration of the linear triatomic CO_2 molecule.

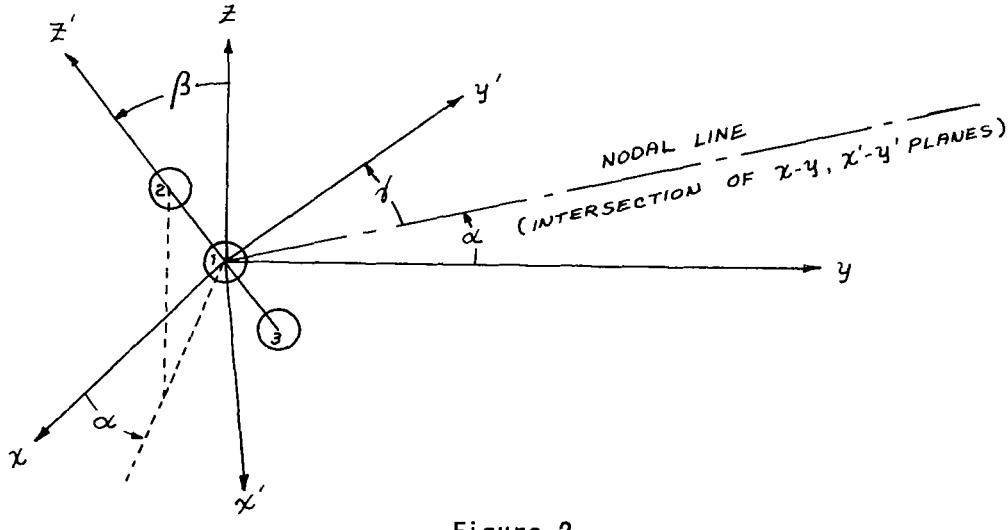

Figure 2

α and β are the azimuthal and polar angles defining the location of the equilibrium molecular axis, and suffice to describe the rotational motion of the molecule, since, (approximation 5 above), the molecule will be treated as a rigid rotator. [The additional coordinates of Fig. 2 are reserved for the description of the bending vibrational motion of the molecule, in Section 2.4 below] .

Using the coordinates of Figs. 1 and 2, the classical Hamiltonian governing the external translational and rotational motion may be written:

$$H_e = \frac{1}{2MR^2}\left(R^2 P_R^2 + P_\Theta^2 + \sin^{-2}\Theta P_\Phi^2\right) + \frac{1}{2I}\left(P_\beta^2 + \sin^{-2}\beta\, P_\alpha^2\right) + V_o\left(R, \Theta, \Phi, \alpha, \beta\right) \tag{2.1}$$

$$P_R = M\dot{R}\,, \quad P_\Theta = MR^2\dot{\Theta}\,, \quad P_\Phi = MR^2\sin^2\Theta\,\dot{\Phi}\,,$$

$$P_\beta = I\dot{\beta}\,, \quad P_\alpha = I\dot{\alpha}\sin^2\beta\,,$$

where M is the reduced mass of the CO_2 - M system, I is the moment of inertia of the CO_2 molecule, and V_o is the zeroth approximation to the CO_2 - M intermolecular potential; its explicit form is derived in the following section.

The Hamiltonian of Eq. (2.1) is used to form canonical equations of motion, governing the collision of an atom and a (triatomic) rigid rotator. For specified initial trajectory parameters, these equations can be solved numerically by machine computation, obtaining the time variation of the trajectory coordinates R, Θ, Φ, α, β during the course of a CO_2 - M collision.*

2.3 INTERMOLECULAR POTENTIAL

As stated above, we take this potential to be a linear combination of

*Details of these machine solutions are given in a previous report, CAL No. AM-2438-A-1.

three point-center interactions

$$V(r_i) = \sum_{i=1}^{3} V_i(r_i) \tag{2.2}$$

For the purposes of discussion, it is assumed that r_i represents the distance from the incident particle to the i^{th} nucleus of the CO_2 molecule. However, as will be discussed below, the resulting potential can be parametrically varied to account for interactions not centered on the nuclei.

We have chosen, for the V_i, simple exponential interactions. In particular, for V_1, the potential centered on the carbon nucleus, we choose a linear combination of attractive and repulsive exponentials

$$V_1 = C_1 e^{-\alpha_1 r_1} - C_4 e^{-\alpha_4 r_1} \tag{2.3}$$

For V_2, V_3 simple exponential repulsive interactions are taken

$$V_2 = C_2 e^{-\alpha_2 r_2}, \qquad V_3 = C_3 e^{-\alpha_3 r_3} \tag{2.4, 2.5}$$

The distances r_i can be written in terms of the coordinates of Figs. 1 and 2, and the vibrational displacement coordinates of the CO_2 molecule. The complete result is cumbersome, and will not be quoted here. However, if, following Takayanagi[9], we expand the potential Eq. (2.2) about the equilibrium positons of the nuclei, the dependence of these potential terms on the vibrational coordinates can be displayed explicitly. The result of this procedure is

$$\begin{aligned} V = {} & C_1 e^{-\alpha_1 R} - C_4 e^{-\alpha_4 R} \\ & + \sum_{i=2,3} C_i e^{-\alpha_i \rho_i} \\ & + \sum_{i=1}^{3} f_i S_i + \sum_{i,j=1}^{3} q_{ij} S_i S_j + \cdots \end{aligned} \tag{2.6}$$

Here, ρ_2, ρ_3 are the equilibrium (non-vibrating) separations of the incident particle from the oxygen nuclei of the CO_2 molecule:

$$\rho_2 = \left[R^2 + \ell^2 + 2\ell R \cos\Theta'\right]^{1/2} \tag{2.7a}$$

$$\rho_3 = \left[R^2 + \ell^2 - 2\ell R \cos\Theta'\right]^{1/2}; \tag{2.7b}$$

ℓ is the equilibrium C - O separation, and Θ' is the angle between $\bar{R}$ and the molecular axis:

$$\cos\Theta' = \cos\beta\cos\Theta - \sin\alpha\sin\Theta\sin(\beta - \Phi)$$

The coefficients f_i, g_{ij}, etc. are functions of the external coordinates $R, \Theta, \Phi, \alpha, \beta, \gamma$ only.

The terms on the first line of this potential, Eq. (2.6), cause purely elastic scattering, being functions of the translational coordinate only. The terms on the second line give rise to rotational transitions, while the remaining terms create simultaneous rotational-vibrational transitions. It is seen that rotational excitation can be treated independently of vibrational excitation, but if one retains the effect of vibrational structure in the potential, one must also treat rotational interactions to maintain a consistent level of approximation.

The first three terms in this potential are similar to the potential adopted by Parker[30] to calculate rotational relaxation times for diatomic molecules. Parker, however, did not require all his potentials to be centered on the nuclei but allowed the 2, 3 potential centers to be closer to the mass center along the molecular axis to account for the repulsive interaction of the electron cloud. This procedure corresponds to letting ℓ in Eq. (2.7a, b) be a variable parameter which can be less than the equilibrium C-O separation. Raff[31] has shown that the procedure gives rotational excitation cross sections which can be in good agreement with calculations based on more exactly determined potentials for simple systems such as H_2-H_e. Thus, although it is acknowledged that pairwise potentials, such as Eq. (2.2), centered on the nuclei, are not entirely satisfactory, one can approximate the true potential by letting ℓ be a variable parameter.

The decoupling approximation used in the solutions for the external motion outlined in Section 2.2 above corresponds to the neglect of the potential terms in Eq. (2.6) which involve the vibrational coordinates. Thus the potential V_o used in the Hamiltonian, Eq. (2.1), is given by the first two lines

of Eq. (2.6):

$$V_o = C_1 e^{-\alpha_1 R} - C_4 e^{-\alpha_4 R} + \sum_{i=2,3} C_i e^{-\alpha_i \rho_i}$$

2.4 INTERNAL VIBRATIONAL MOTION

A quantum mechanical description of the CO_2 vibrational motion is used. The quantum mechanical Hamiltonian operator for CO_2 vibration is written:

$$H_v = H_1 + H_2$$

where H_1 is the operator for the normal mode CO_2 description:

$$H_1 = \frac{\hbar^2}{2}\left\{\frac{1}{\mu_1}\frac{\partial^2}{\partial S_1^2} + \frac{1}{\mu_2}\left[\frac{1}{S_2}\frac{\partial}{\partial S_2}\left(S_2\frac{\partial}{\partial S_2}\right) + \frac{1}{S_2^2}\frac{\partial^2}{\partial \gamma^2}\right] + \frac{1}{M_3}\frac{\partial^2}{\partial S_3^2}\right\}$$

$$- \frac{1}{2}\left[\mu_1\omega_1^2 S_1^2 + \mu_2\omega_2^2 S_2^2 + \mu_3\omega_3^2 S_3^2\right] \qquad (2.8)$$

and H_2 are the first order anharmonicity terms:

$$H_2 = \alpha_{111} S_1^3 + \alpha_{122} S_1 S_2^2 + \alpha_{133} S_1 S_3^2 \qquad (2.9)$$

Here, S_1 is the symmetric stretching displacement. $S_1 + 2\ell$ is the displacement of the two O atoms relative to each other.

S_2, γ are the bending displacement coordinates. S_2 and γ are the cylindrical coordinates of the displacement of the C atom relative to the line joining the two atoms. This distance is measured perpendicular to the equilibrium figure axis (i.e., the z' axis of Fig. 2). Note that, with reference to Fig. 2, the x' - z' plane is defined as the plane of the bending motion of the molecule; S_2 is in this plane, and γ specifies the orientation of this plane about the molecular (z') axis relative to the nodal line in Fig. 2.

S_3, the asymmetric stretching displacement, is the displacement of the C atom along the equilibrium figure axis relative to the center of mass of the O atoms.

The solution of the Schrodinger equation for the operator H_1 ,

$$H_1 \psi^{(o)} = E \psi^{(o)}$$

yields the normal mode wave functions $\psi_n^{(o)}$ and energies $E_n^{(o)}$ for the CO_2 molecule. It is a principal feature of CO_2, however, that the observed IR and Raman spectra are not entirely consistent with such a purely normal-mode model of the vibrational energy states. The energies of some kinetically important CO_2 states can be predicted only if one considers anharmonicity coupling between normal-mode states having comparable energies. This mechanism is the well-known Fermi resonance coupling, and it gives rise to a "mixing" of some of the normal-mode vibrational wave functions. For an adequate description of these Fermi resonance states, the anharmonicity terms H_2 must be included. The solution of the Schrodinger equation with the inclusion of anharmonic coupling:

$$H_v \psi = (H_1 + H_2) \psi = E \psi , \tag{2.10}$$

is treated in standard references[32, 33, 34] where wave functions and energy levels are obtained using first order time-independent perturbation theory for degenerate levels. The wave functions, ψ_n , are found, to zeroth order in the approximation, to be linear combinations of the normal mode wave functions:

$$\psi_n \approx \psi_n^{\{o\}} = \sum_{k=0}^{q} C_{nk}^{(o)} \psi_k^{(o)} , \tag{2.11}$$

where q is the order of the Fermi resonance degeneracy, and the normal mode wave functions $\psi_n^{(o)}$ are given by:

$$\psi_n^{(o)} = u_1(r_1)\, u_3(r_3)\, R^{v_2 \ell}(r_2)\, e^{\pm i \ell \gamma} \tag{2.12}$$

Here, $u(r_i)$ are the standard SHO wave functions:

$$u_i(r_i) = N_{v_i} e^{-\frac{1}{2} r_i^2} \tilde{H}_{v_i}(r_i) ,$$

$$N_{v_i}^2 = \frac{1}{\sqrt{\pi}\, 2^{v_i} V_i!} \quad , \qquad r_i = \left(\frac{\omega_i \mu_i}{\hbar}\right)^{1/2} S_i$$

$\tilde{H}_{v_i}(r_i)$ is the V_i^{th} Hermite polynomial of argument r_i .

The remaining part of the wave function, $R^{v_2 l}(r_2) e^{\pm i l \gamma}$, is the solution for the two-dimensional isotropic harmonic oscillator in polar coordinates (r_2, γ):

$$R(r_2)^{v_2 l} e^{\pm i l \gamma} = [k!]^{1/2} [(l+k)!]^{-1/2} \pi^{-1/2} r_2^l e^{-r_2^2/2} L_k^l(r_2^2) e^{\pm i l \gamma},$$

where $k \equiv (V_2 - l)/2$. $L_k^l(r_2^2)$ is the associated Laguerre polynomial of argument, r_2^2 .

The $C_{n_k}^{(o)}$'s are found using standard time-independent perturbation theory for degenerate levels. The $C_{n_k}^{(o)}$'s are so chosen that the wave functions $\psi_n^{\{o\}}$ are orthonormal.

The energy levels for the lower CO_2 states are shown in Fig. 3 . The wave functions corresponding to the lowest fifteen states are given in Table 2.1. The states in Fermi resonance are linked by braces.

We now consider the behavior of the above system under the action of the time-dependent perturbation potential:

$$V = V_o(t) + \sum_{i=1}^{3} f_i(t) S_i + \sum_{i,j=1}^{3} q_{ij}(t) S_i S_j + \cdots \qquad (2.13)$$

As mentioned previously, in the present model, the influence of a collision is represented by a potential of this form. Eq. (2-13) is the interaction potential Eq. (2.6). In Eq. (2.6), V_o , f_i , and q_{ij} are functions of the collision trajectory variables, R , Θ , Φ , α , β . In Eq. (2-13), V_o, f_i , q_{ij} are written as explicit functions of time, the time dependence of the trajectory variables bring obtained from solution of the equations of motion for the collision trajectory, as discussed in Section 2.2.

Using standard methods, the solution of the wave equation for the perturbed system:

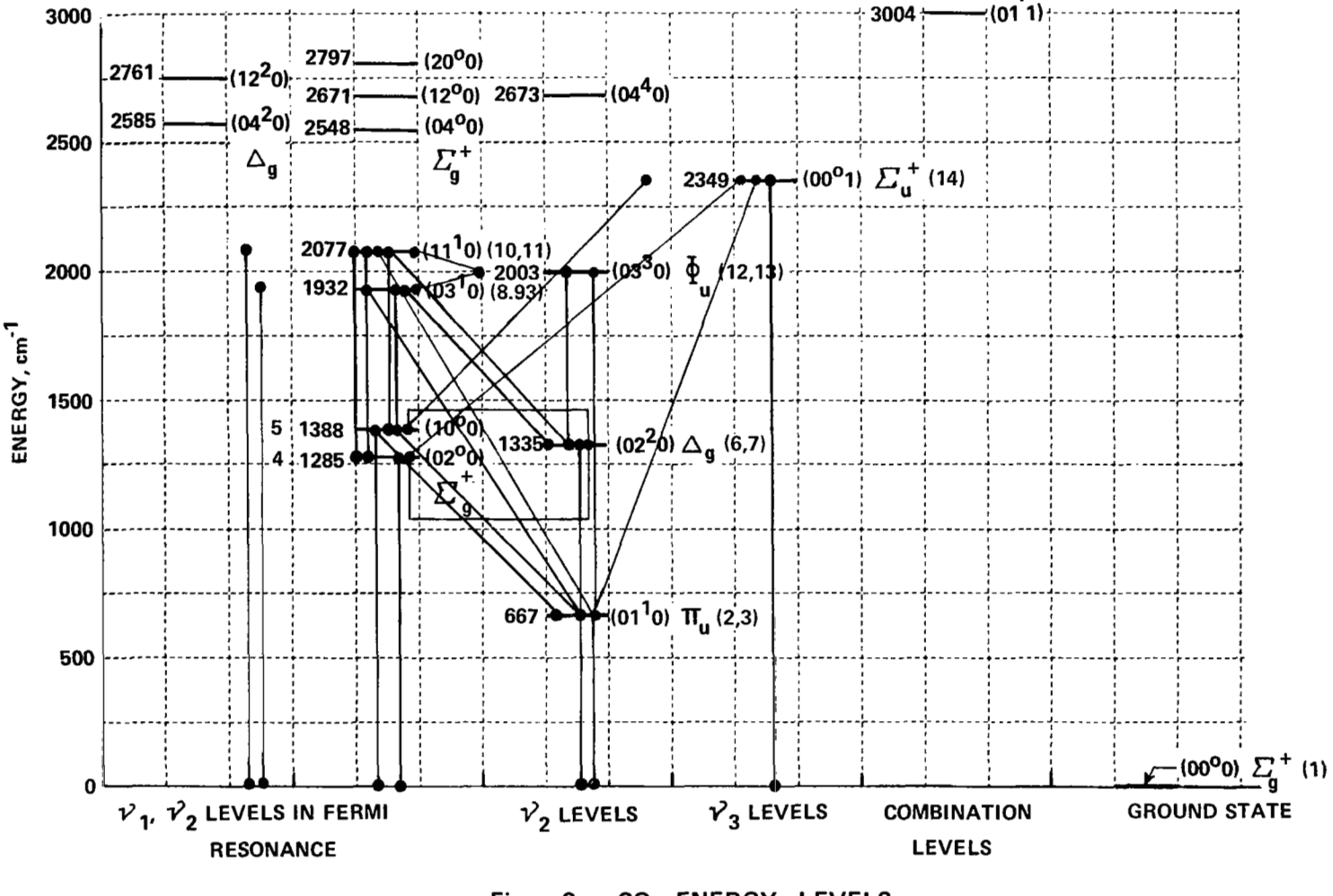

Figure 3 CO_2 ENERGY LEVELS

Table 2.1

CO_2 WAVE FUNCTIONS

State Designation		Wave Functions	Energy, cm^{-1}
n	$(V_1\ V_2^{\ell}\ V_3)$	$\psi_n^{\{o\}} / \psi_o^{\{o\}} = \pi_e^{\frac{1}{2}(r_1^2 + r_2^2 + r_3^2)} \psi_n^{\{o\}}$	E_n
0	$(0\ 0^{\circ}\ 0)$	1	0
1	$(0\ 1^{1}\ 0)$	$r_2\, e^{\pm i\gamma}$	667
2	$(0\ 2^{\circ}\ 0)$	$0.648\sqrt{2}\ r_1 - 0.766\ (1 - r_2^2)$	1285
3	$(1\ 0^{\circ}\ 0)$	$0.766\sqrt{2}\ r_1 + 0.648\ (1 - r_2^2)$	1388
4	$(0\ 2^{2}\ 0)$	$\frac{1}{\sqrt{2}}\ r_2^2\ e^{+- 2i\gamma}$	1335
5	$(0\ 3^{1}\ 0)$	$0.743\ \frac{1}{\sqrt{2}}\ (2 r_2 - r_2^3)\, e^{\pm i\gamma} + 0.669\sqrt{2}\ r_1 r_2\, e^{\pm i\gamma}$	1932
6	$(1\ 1^{1}\ 0)$	$0.669\ \frac{1}{\sqrt{2}}\ (2 r_2 - r_2^3)\, e^{\pm i\gamma} - 0.743\sqrt{2}\ r_1 r_2\, e^{\pm i\gamma}$	2077
7	$(0\ 3^{3}\ 0)$	$\frac{1}{\sqrt{6}}\ r_2^3\ e^{\pm 3i\gamma}$	2003
8	$(0\ 0^{\circ}\ 0)$	$\sqrt{2}\ r_3$	2349
9	$(0\ 4^{\circ}\ 0)$	$0.620\,(1 - 2r_2^2 + \frac{1}{2} r_2^4) + 0.684\, r_1(1 - r_2^2) + 0.385\,(2 r_1^2 - 1)$	2548
10	$(1\ 2^{\circ}\ 0)$	$0.577\,(1 - 2r_2^2 + \frac{1}{2} r_2^4) - 0.065\, r_1(1 - r_2^2) - 0.814\,(2 r_1^2 - 1)$	2671
11	$(2\ 0^{\circ}\ 0)$	$0.532\,(1 - 2r_2^2 + \frac{1}{2} r_2^4) - 0.726\, r_1(1 - r_2^2) + 0.435\,(2 r_1^2 - 1)$	2797
12	$(0\ 4^{4}\ 0)$	$1 - 2 r_2^2 + \frac{1}{2} r_2^4$	2673
13	$(0\ 4^{2}\ 0)$	$0.747\,(3 r_2^2 - r_2^4)\, e^{\pm 2i\gamma} + 0.665\, r_1 r_2^2\, e^{\pm 2i\gamma}$	2585
14	$(1\ 2^{2}\ 0)$	$0.665\,(3 r_2^2 - r_2^4)\, e^{\pm 2i\gamma} - 0.747\, r_1 r_2^2\, e^{\pm 2i\gamma}$	2761

$$(H_v + V)\,\Psi = i\hbar\,\frac{\partial \Psi}{\partial t} \tag{2.14}$$

can be rephrased in a completely equivalent way as a problem in finding the coefficients $b_{mn}(t)$, where

$$\Psi_m = \sum_n b_{nm}(t)\,\psi_n^{\{o\}}\,e^{-iE_n t/\hbar} \tag{2.15}$$

$\psi_n^{\{o\}}$ are the combination wave functions given by Eq. (2.11). The coefficients b_{mn} are determined exactly by the solution of the first order equations:

$$\dot{b}_{mn} = -\frac{i}{\hbar}\sum_k \langle n|V|k\rangle\, b_{mk}\, e^{i\omega_{nk}t} \tag{2.16}$$

$$n = 0, 1, 2, \cdots$$

where

$$\langle n|V|k\rangle \equiv \int_{\gamma=0}^{2\pi}\int_{r_3=-\infty}^{\infty}\int_{r_2=0}^{\infty}\int_{r_1=-\infty}^{\infty} \psi_n^{\{o\}*}\, V\, \psi_k^{\{o\}}\, r_2\, dr_1\, dr_2\, dr_3\, d\gamma\ , \tag{2.17}$$

$$\omega_{nk} \equiv (E_n - E_k)/\hbar$$

Equations (2.16) are the so-called interaction representation, and are completely equivalent to the wave equation, Eq. (2.14), no small perturbation approximation having been introduced. If the CO_2 molecule is initially in state m before collision ($t = -\infty$), $P_{mn}(t) = |b_{mn}(t)|^2$ is the probability that it will be in state n at time t.

2.5 THERMAL AVERAGING OF TRANSITION PROBABILITIES

The transition probabilities P_{mn} obtained from solution of Eqs. (2.16) are functions of the initial trajectory conditions. With reference to Figures 1 and 2, one can select a particular collision trajectory by specifying the initial position of the incoming structureless particle in spherical coordinates (R_o, Θ_o, Φ_o), the initial orientation of the CO_2 molecule (α_o, β_o), the initial rotational velocity of the CO_2 molecule, and the initial relative velocity $\vec{V}_o$ between the molecules. Here the subscript zero has been used to indicate the initial values for the coordinates. Transition probabilities calculated from Eq (2.16) must be incorporated into an expression for the

thermally averaged probability of $m \to n$ transitions in the gas, for comparison with typical vibrational relaxation experiments. Such an averaged probability involves integration over a thermal distribution of collision trajectories specified by (R_o , Θ_o , Φ_o , α_o , β_o), and the initial relative translational and rotational velocities. However, the coordinate system of Figs. 1 and 2 is completely arbitrary in orientation and is not the most convenient one to use for the quadrature. Consequently, for thermal averaging a second coordinate system (dependent upon the parameters of the collision) has been chosen such that the xy -plane is coincident with the plane determined by the line joining the centers of the two molecules (i.e. the direction specified by (R_o , Θ_o , Φ_o) above) and by the initial relative velocity $\vec{V}_o$. The orientation of this new coordinate system is completely specified if we choose the x -axis to be parallel, but oppositely directed to $\vec{V}_o$.

In this new coordinate system the incoming structureless particle appears as shown in Fig. 4. Now the initial parameters needed to specify the interaction are six in number: the magnitude of the incoming relative velocity V_o , the impact parameter b for the collision, the orientation (α_o , β_o) of the axis of the CO_2 molecule (now referred to the new coordinate system, but measured in the same fashion as shown in Fig. 2), and the angular velocity (ω_{α_o}, ω_{β_o}) of the CO_2 molecule. (Note that only two components are required to specify the angular velocity vector since this vector is orthogonal to the CO_2 molecular axis.)

One further alteration is needed to simplify the selection of the initial parameters for each collision trajectory. Rather than specify the initial angular velocity of the CO_2 molecule by the parameters ω_{α_o} and ω_{β_o} , we choose the magnitude p of the angular momentum and an angle $\tilde{\gamma}$ defining the direction of the angular momentum in phase space. ω_{α_o} and ω_{β_o} are found from p and $\tilde{\gamma}$ as follows:

$$\omega_{\alpha_o} = \frac{1}{I} p \sin\tilde{\gamma} \sin\beta_o$$

$$\omega_{\beta_o} = \frac{1}{I} p \cos\tilde{\gamma}$$

In terms of these coordinates, it can be shown that the thermally averaged probability of a transition from state m to state n is:

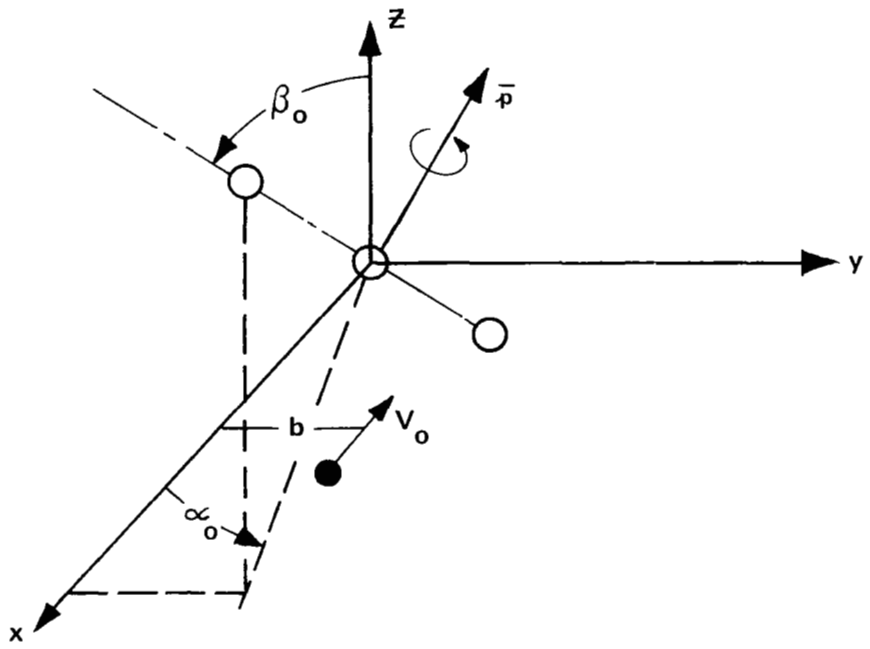

Figure 4 INITIAL TRAJECTORY ORIENTATION

$$P_{mn}(T) = \frac{1}{2}\left(\frac{M}{kT}\right)^2 \frac{1}{(2\pi)^2 I kT}\int_0^\infty \exp\left[-\frac{MV_o^2}{2kT}\right] V_o^3\, d\, V_o \int_0^{b_*} 2\,\frac{b}{b_*}\,\frac{db}{b_*} \qquad (2.18)$$

$$\int_0^\pi \sin\beta_o\, d\,\beta_o \int_0^\pi d\,\alpha_o \int_0^{2\pi} d\,\tilde{\gamma} \int_0^\infty p\, d\, p\, \exp\left[-p^2/2IkT\right] P_{mn} \,,$$

where T is the gas kinetic temperature and P_{mn} is found from the solution obtained from Eqs. (2.16).

2.6 SOLUTIONS

The model developed in the preceding sections retains a large degree of generality. In particular, the model includes the geometrical dependence of collisional excitation of the various CO_2 vibrational modes, the influence of molecular rotation, anharmonic coupling among the vibrational modes, and the influence of multistate transition processes. Within the framework of this formalism, certain specific problems of CO_2 collisional excitation have been chosen for detailed numerical solution. In each case chosen, Eqs. (2.16) and for Eq. (2.18) can be further simplified, permitting more economical machine calculation times. Two major problem areas have been selected: 1.) collision-induced vibration-to-vibration (V-V) energy transfer among the CO_2 modes, and, 2.) the role played by geometrical and rotational effects in the collisional excitation of CO_2, i.e., translation-to-vibration (T-V) energy transfer. The calculations involving problem 1) have been made only for certain restricted geometrical orientations, while retaining all coupling terms presented in Section 2.4. The calculations for problem 2) have been over the complete distribution of trajectory parameters (V_o, p_o, b, α_o, β_o, $\tilde{\gamma}_o$) given in Section (2.5), but with the elimination of second order terms which couple the vibrational modes; this yields a normal-mode model in which the T-V excitation of each mode can be treated independently. In the following sections, calculations performed in both problem areas are presented.*

* Considerably more space is devoted to the V-V calculations; details of the T-V calculations have been given in a previous report (CAL No. AM-2438-A-1) and will also be published separately.

3. INTERMODE (V-V) ENERGY TRANSFER

3.1 GENERAL

To perform a calculation of collision-induced V-V energy transfer among the CO_2 modes, Eqs. (2.16) have been programmed directly for machine solution. A Runge-Kutta-Merson fourth order integration technique, programmed in Fortran language, was used. The calculation can include the fifteen states listed in Table 2.1, which contains all CO_2 states having a characteristic temperature $\leq$ 4000°K. These include the principal CO_2 levels participating in the 9.6 μ and 10.6 μ CO_2 laser transitions.

The following types of controls and checks were used to insure accuracy of the integration procedure:

1. A local truncation error of 10^{-6} was specified for each integration step; at no time was this exceeded.

2. The maximum allowable time-step size was greatly reduced to force integration over smaller intervals in the vicinity of the classical turning point; no significant change in the calculated transition probabilities was observed.

3. The trajectory calculations were extended over sufficient intermolecular separation to insure that the transition probabilities asymptoted to constant values, i.e., the calculations were extended to ranges where all significant molecular interaction ceased.

4. For the present model, a statement of detailed balancing assumes the form:

$$P_{mn}(V_o, \rho_o, b, \alpha_o, \beta_o, \tilde{\gamma}_o) = P_{nm}(V_o, \rho_o, b, \alpha_o, \beta_o, \tilde{\gamma}_o)$$

i.e., for a given trajectory, characterized by the parameters V_o, ρ_o, etc., $P_{mn} = P_{nm}$. Therefore, runs were made with the same classical trajectory, but using different initial vibrational states. The preceding statement of detailed balance was always satisfied to at least three significant figures for the trajectories checked.

Machine solution of interaction representation equations, similar to (2.16), has been reported in the series of papers by Rapp and Sharp.[35,36] This calculation modeled the colinear collision of a harmonic oscillator and

an atom, and is a systematic study of multistate effects in high energy diatomic molecular collisions. In the present calculation, the coupling between the various CO_2 modes, the nonuniform spacing of the vibrational energy levels, and the anisotropy of the interaction potential give rise to features of the results not present in the colinear, harmonic oscillator case. In the following discussion, comparison will be made with the standard harmonic oscillator behavior reported by Rapp and Sharp.[36]

The matrix elements $\langle n|V|k\rangle$ appearing in Eq (2.16) were evaluated through second order terms in V, Eq (2.13). Evaluation of the time-dependent coefficients, $f_i(t)$ and $g_{ij}(t)$ is one of the most time-consuming operations in the numerical procedure, since these coefficients must be evaluated at each time interval during the course of the trajectory integration. States directly coupled by non-zero matrix elements are shown in Fig. 3; the order of the first non-zero coupling is indicated.*

Two significant features of these couplings should be noted:

1. Collision-induced transitions are possible even between pairs of states for which $\langle n|V|k\rangle = 0$. This is a feature of the multistate nature of the present calculation; only for a first order perturbation approximate solution of Eq (2.12) would $\langle n|V|k\rangle = 0$ disallow an $n \rightarrow k$ transition. In the present calculation, a transition between such a pair of states occurs via transition paths through other, coupled states, which provide an indirect coupling between the initial and final states. This aspect of a multistate calculation, which has been studied extensively when applied to collisional excitation of harmonic oscillator diatomic molecules, is essential in calculations for a polyatomic molecule such as CO_2. As shown in some of the results presented below, many of the most important V-V energy transfer paths are through intermediate states. The near-degeneracy of several CO_2 energy levels make this effect important even at relatively low collisional velocities where a first order perturbation treatment would be adequate in treating excitation of a single harmonic oscillator.

* For the sake of clarity, couplings involving states above 2500 cm^{-1} have been omitted in Fig. 3.

2. Fig. 3 shows the states coupled by nonzero matrix elements. However, transitions between states are a function of initial molecular orientation before collision. The angular dependence of the coefficients f_i, g_{ij} makes many of the couplings small or zero for some orientations. For example, many energy transfer paths involving bending mode states are blocked for purely colinear CO_2-M collisions, i.e., when the collision partner approaches the molecule along the equilibrium molecular axis.

Three initial vibrational configurations have been chosen for extended calculation. These configurations are for the molecule initially in the (01^10), the (00°1), and the (10°0) states. These calculations have been restricted to coplanar orientations ($\Theta = \beta = \frac{\pi}{2}$) zero impact parameter ($b = 0$), and for the molecule initially nonrotating ($\omega_{\alpha_0} = 0$). Molecular constants appropriate for CO_2 - Ar collision were generally used; Table 3.1 gives a summary of these.

TABLE 3.1

MOLECULAR CONSTANTS USED FOR CO_2 - Ar COLLISIONS

I = CO_2 moment of inertia = 7.167×10^{-39} gm cm^2

M = CO_2 - Ar reduced mass = 3.477×10^{-23} gm

M_c = Mass of carbon atom = 1.99×10^{-23} gm

M_o = Mass of oxygen atom = 2.66×10^{-23} gm

Intermolecular potential constants (Eqs (2.5a) - (2.5c)):

$\alpha_1 = \alpha_2 = \alpha_3 = 5 \times 10^8$ cm^{-1}

$\alpha_4 = 0$

$C_1 = C_2 = C_3 = 2.019 \times 10^{-6}$ ergs

$C_4 = 0$

ℓ = Potential anisotropy = 1.16×10^{-8} cm

3.2 ENERGY TRANSFER FROM THE (01^10) BENDING MODE STATE

Calculations were made for the CO_2 molecule initially in the (01^10) state. As mentioned above, a coplanar orientation was used; and all calculations were for the molecule initially non-rotating ($\omega_{\alpha_o} = 0$) and for zero impact parameter ($b = 0$). The initial angular orientation of the molecule (α_o) was systematically varied, as was the initial relative velocity, V_o. These runs were made with the lowest nine coupled states listed in Table 2.1. It was found that the inclusion of this number of states was usually sufficient for accurate calculation at the collision energy range of interest. A discussion of the number of coupled states required for convergence in the CO_2 calculation is given in Section 3.5.

Figure 5 shows the evolution of some selected probability amplitudes ($P_{mn}(t) \equiv |b_{mn}(t)|^2$) during the course of a typical collision trajectory. $P_{mn}(t)$ for various transitions are plotted against time ($t = 0$ at the initial molecular separation of 7.5Å). Approximate CO_2 - Ar separation in angstroms is indicated beside the time scale. The gross behavior of the probabilities, for this particular orientation, is the same as that observed by Sharp and Rapp.[36] The probability of states other than the initial state (01^10) being occupied is much greater in the region of the classical turning point (indicated as "T. P." in the figure) than at the end of the interaction. Maximum probabilities occur shortly after the turning point. It can be noted that probabilities, which, at the end of the trajectory, are less than 10% of the $(01^10) \longrightarrow (000)$ probability, can be a very large fraction of $P_{(01^10) \longrightarrow (000)}$ near the turning point. For this reason, such states must generally be included in calculating $P_{(01^10) \longrightarrow (000)}$, although the probability of a direct transition to them is small at the end of the interaction.

Due to the symmetrical, broadside orientation of the collision whose results are shown in Fig. 5, the CO_2 molecule was not set into rotation by the collision. For other orientations, where the molecule may be rotating, the shape of the probability curves may differ; in some cases, a second peak occurs in the vicinity of the turning point.

The states in Fermi resource are linked by brackets. Despite the mixing of such states, the probabilities for transition to them may differ considerably.

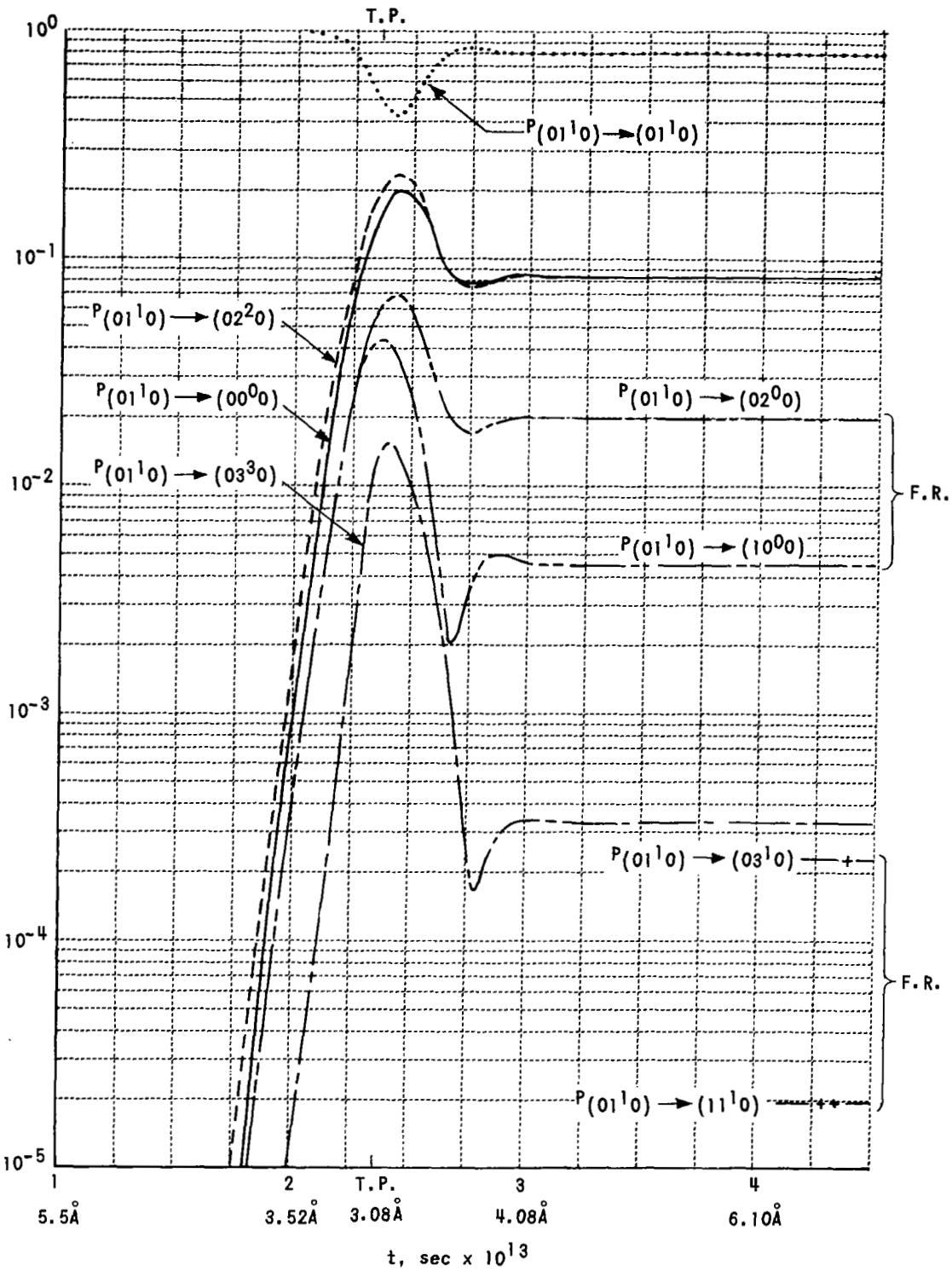

Figure 5 TIME EVOLUTION OF CO_2 PROBABILITY AMPLITUDES DURING COLLISION. MOLECULE INITIALLY IN (01^10) STATE.

The potential anisotropy (ℓ = 1.16Å) is considerable in these calculations, and the probabilities show significant structure when plotted against initial orientation, α_o , as in Fig. 6. In the present case of energy transfer involving a bending mode state, the colinear orientation ($\alpha_o = 0$) is generally unfavorable for creating vibrational transitions. For those transitions plotted in Fig. 6, the broadside orientation, $\alpha_o = \frac{\pi}{2}$, is most favorable at the indicated relative velocity (V_o = 2 x 10^5 cm/sec). However, for transitions to compound states involving stretching modes, such as $(01^10) \longrightarrow (11^10)$, the most favorable orientation can be at some intermediate value of α_o .

The present calculations provide information on the extent of intermode vibrational coupling in CO_2 , which can be useful in kinetic modeling of high temperature CO_2 processes. In Figs. 7 and 8, the calculated transition probabilities have been averaged over orientation and a Maxwellian distribution of relative translational velocities. From Eq(2.18), we have, for the thermally averaged transition probability:

$$P_{mn}(T) = \frac{1}{\pi}\left(\frac{M}{kT}\right)^2 \int_o^\infty e^{-MV_o^2/2kT} V_o^3 \, dV_o \int_o^{\pi/2} d\alpha_o \, P_{mn}(\alpha_o, V_o), \tag{3.1}$$

where T is the translational temperature. The probabilities so calculated are somewhat smaller than if the average were extended over impact parameter, initial rotational velocity, and out-of-plane orientations, as indicated by the calculations of Section 4.2 below. The relative values of the transition probabilities, however, should not be significantly affected by neglect of these effects.

Figure 7 illustrates the close coupling between the bending and the symmetric stretch modes. The probability for energy transfer from (01^10) to the symmetric stretch states, such as the Fermi resonance pair (10°0) and (02°0), is of the same magnitude as the probability for the direct excitation of the bending mode, $(00^\circ 0) \longrightarrow (01^10)$. Further, the total probability for the excitation of higher states from (01^10) is greater than the probability for the

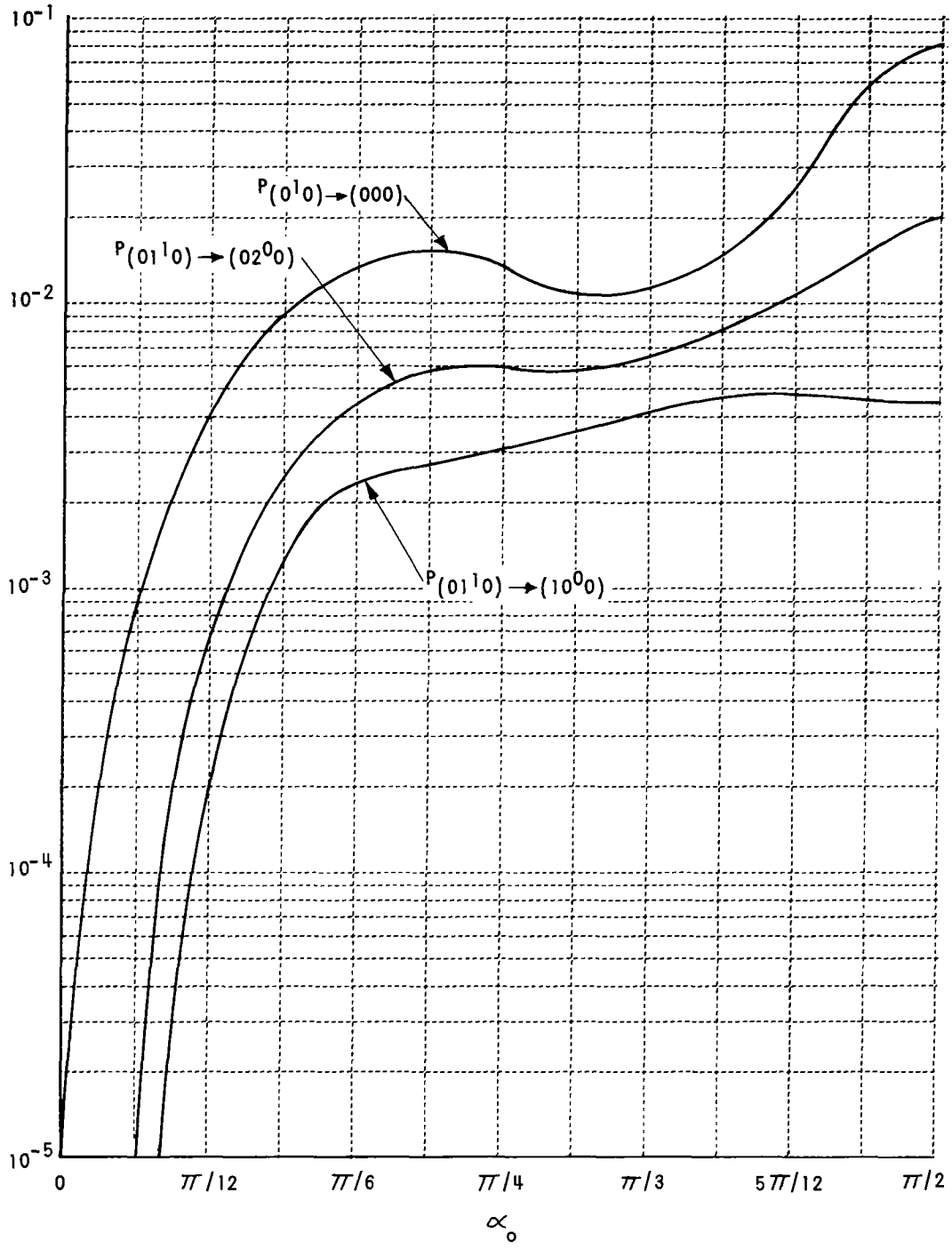

Figure 6 TRANSITIONS FROM (01^10) BENDING STATE VS INITIAL MOLECULAR ORIENTATION. $b = 0$, $V_o = 2 \times 10^5$ cm/sec.

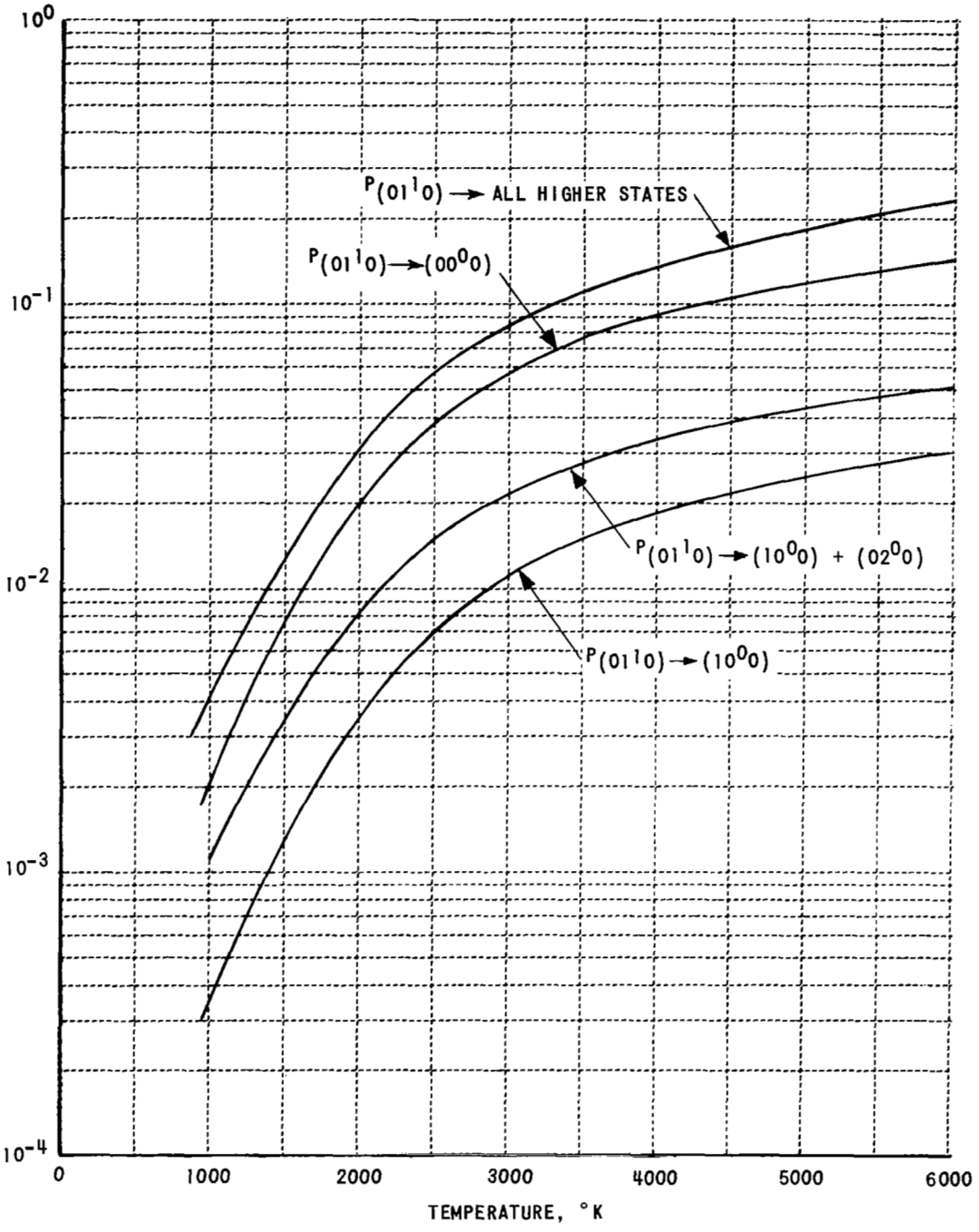

Figure 7 TRANSITIONS FROM (01^10) BENDING STATE VS TEMPERATURE

direct excitation of $(01^{1}0)$ itself. All these probabilities are much larger than the probability for the direct T-V excitation of the symmetric stretch mode, i.e., $(00°0) \longrightarrow (10°0)$. It therefore appears that vibrational excitation of the symmetric stretch states precedes overwhelmingly by the two-step process:

$$CO_2\,(00°0) + M \longrightarrow CO_2\,(01^{1}0) + M$$

followed by:

$$CO_2\,(01^{1}0) + M \longrightarrow CO_2\,(10°0) + M$$

rather than by the direct process:

$$CO_2\,(00°0) + M \longrightarrow CO_2\,(10°0) + M$$

This conclusion is also evident from the distorted wave calculation of Herzfeld,[16] which includes Fermi resonance coupling of the CO_2 states.

The coupling of the $(01^{1}0)$ state with the $(00°1)$ state of the asymmetric stretch mode is much weaker than the $(01^{1}0)$ coupling with symmetric stretch. Figure 8 is a plot of the $(01^{1}0) \longrightarrow (00°1)$ probability against temperature. The values are comparable to those for the direct excitation of this state from ground, i.e., $(00°0) \longrightarrow (00°1)$. Further discussion of energy transfer involving the $(00°1)$ state is given in the following section, which treats $(00°1)$ deactivation.

3.3 ENERGY TRANSFER FROM THE (00°1) ASYMMETRIC STRETCHING STATE

Calculations for deexcitation of the $(00°1)$ state are of particular interest, inasmuch as this is the upper state for the 9.6 and 10.6 micron CO_2 laser transitions. Calculations were performed for both Ar and He as the collision partner, to observe the influence of reduced mass on the calculated transition probabilities.

Runs were again made for the coplanar, initially non-rotating, zero

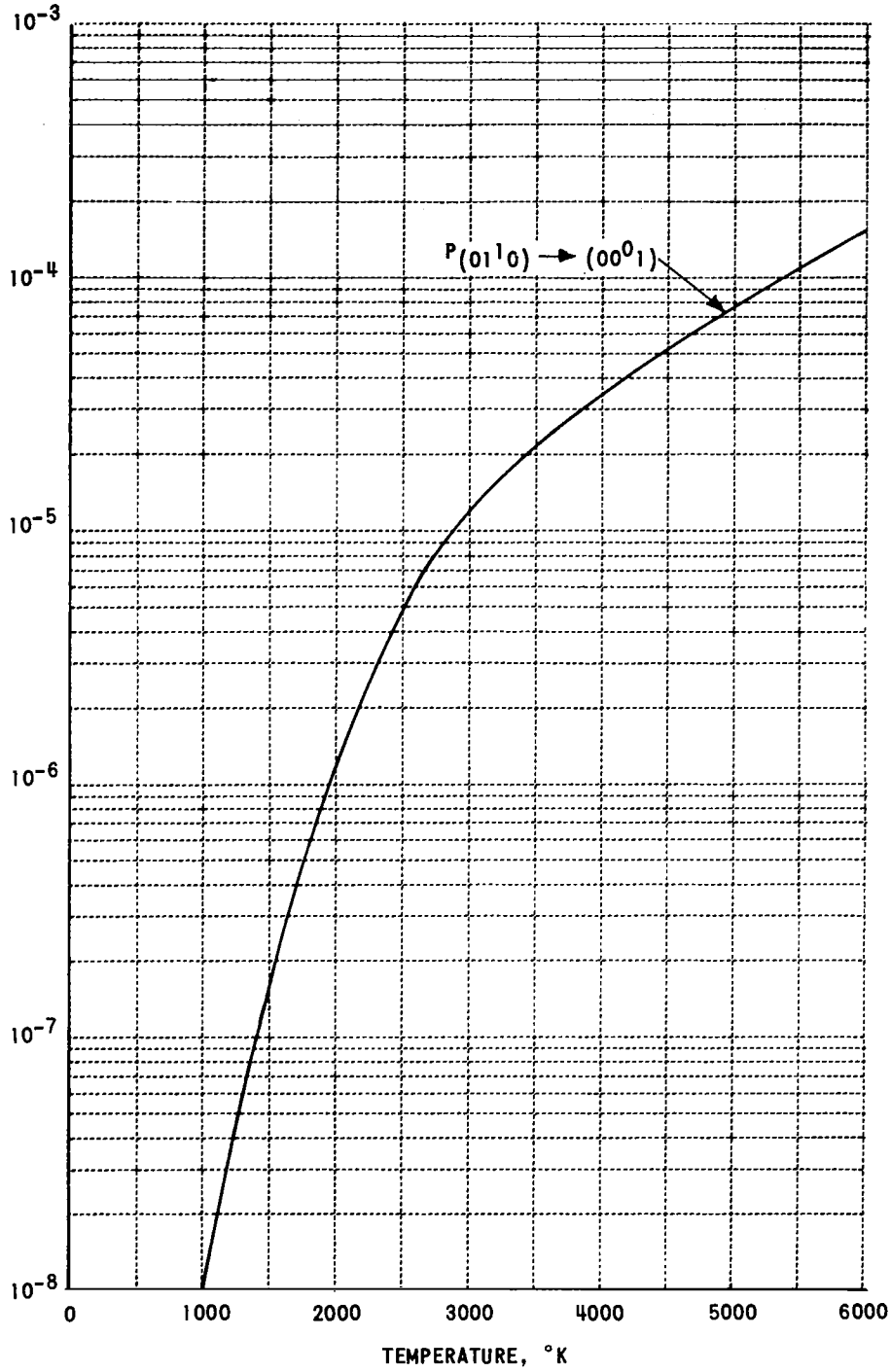

Figure 8 $P_{(01^10)} \rightarrow (00^01)$ TRANSITION VS TEMPERATURE

impact parameter case. It was found that (00°1) deactivation was accomplished primarily by the following energy transfer paths involving ν_1 , ν_2 Fermi resonance pairs and triplets as end states:

$$CO_2\ (00^{\circ}1) + M \longrightarrow CO_2 \begin{Bmatrix} 02^{\circ}0 \\ 10^{\circ}0 \end{Bmatrix} + M$$

$$CO_2\ (00^{\circ}1) + M \longrightarrow CO_2 \begin{Bmatrix} 03^{\circ}0 \\ 11^{\circ}0 \end{Bmatrix} + M$$

$$CO_2\ (00^{\circ}1) + M \longrightarrow CO_2 \begin{Bmatrix} 04^{\circ}0 \\ 12^{\circ}0 \\ 20^{\circ}0 \end{Bmatrix} + M$$

The probabilities for direct deactivation to the ground (00°0) state were negligible, as were the probabilities for deactivation to the isolated bending mode levels $(01^{1}0)$, $(02^{2}0)$, $(03^{3}0)$, $(04^{4}0)$. This conclusion was found to remain valid for any initial orientation of the collision pair.

An interesting feature of the calculation is that the $\begin{Bmatrix} 03^{\circ}0 \\ 11^{\circ}0 \end{Bmatrix}$ and $\begin{Bmatrix} 04^{\circ}0 \\ 12^{\circ}0 \\ 20^{\circ}0 \end{Bmatrix}$ Fermi resonance groups are not directly coupled to the (00°1) state, despite the large probability for transitions to these states. These states are excited primarily by a two-step process involving the $\begin{Bmatrix} 02^{\circ}0 \\ 10^{\circ}0 \end{Bmatrix}$ Fermi resonance levels:

$$CO_2\ (00^{\circ}1) \longrightarrow CO_2 \begin{Bmatrix} 02^{\circ}0 \\ 10^{\circ}0 \end{Bmatrix} \longrightarrow CO_2 \begin{Bmatrix} 03^{\circ}0 \\ 11^{\circ}0 \end{Bmatrix}$$

$$\text{or} \quad CO_2 \begin{Bmatrix} 04^{\circ}0 \\ 12^{\circ}0 \\ 20^{\circ}0 \end{Bmatrix}$$

This process is shown graphically in Fig. 9, which shows the time evolution of the (10°0) and (20°0) probability amplitudes during a typical CO_2 - Ar collision, with the molecule initially in the (00°1) state. Initially, the (10°0) level is excited directly from (00°1). As (10°0) is excited, however, energy begins to be transferred from (10°0) to (20°0); increases in the (20°0) amplitude are mirrored by decreases in the (10°0) amplitude. At the end of the trajectory, both (10°0) and (20°0) are left with a significant probability of excitation. The dominant role of multistate transition paths is apparent.

Figure 10 shows the thermally averaged transition probabilities for (00°1) deactivation, in CO_2 - Ar and CO_2 - He collisions, as functions of temperature. It is seen that the difference between (00°1) deactivation by He collision and by Ar collision is relatively small, the He deactivation

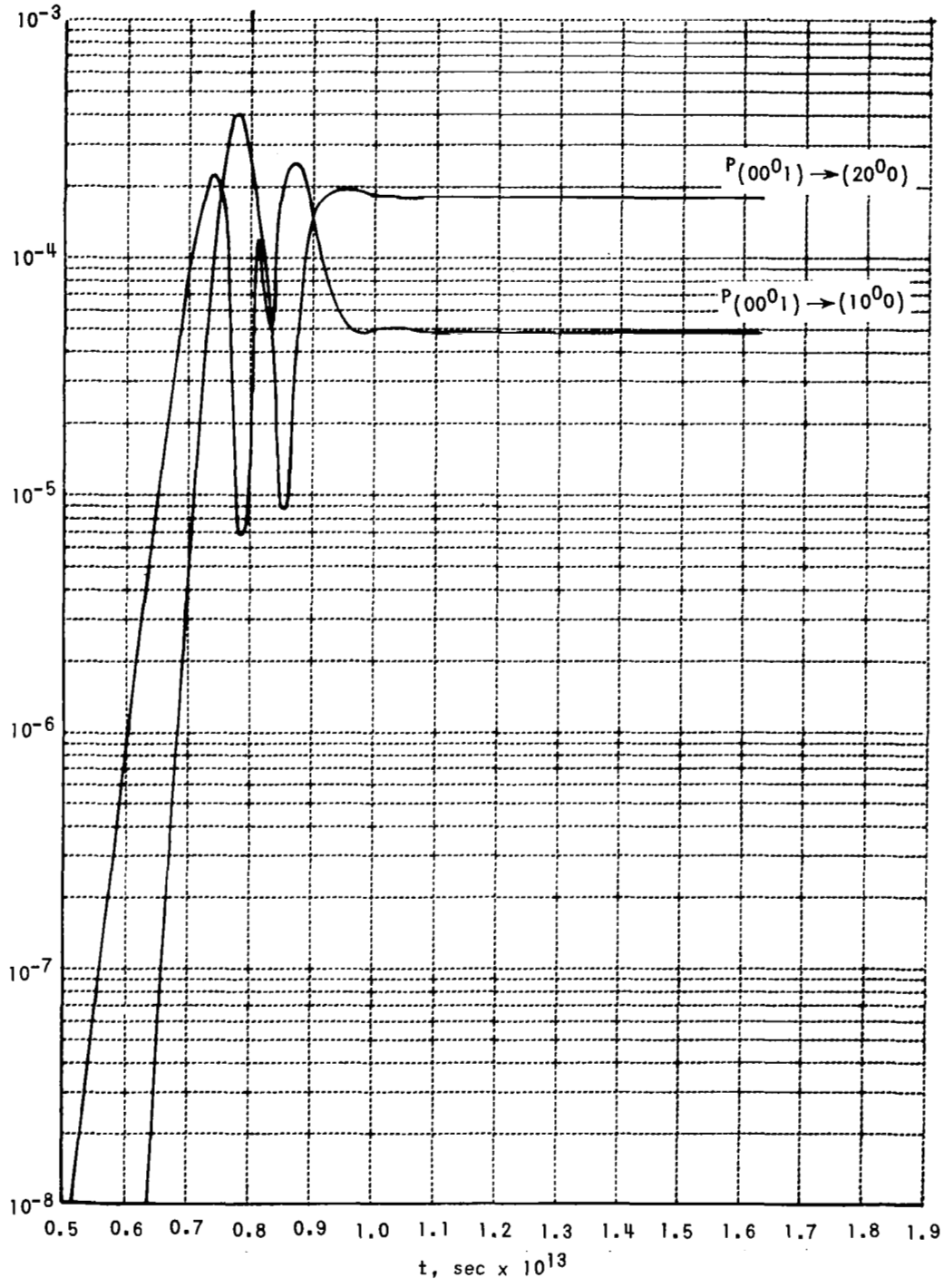

Figure 9 TIME EVOLUTION OF CO_2 PROBABILITY AMPLITUDES DURING COLLISION. MOLECULE INITIALLY IN (00^01) STATE.

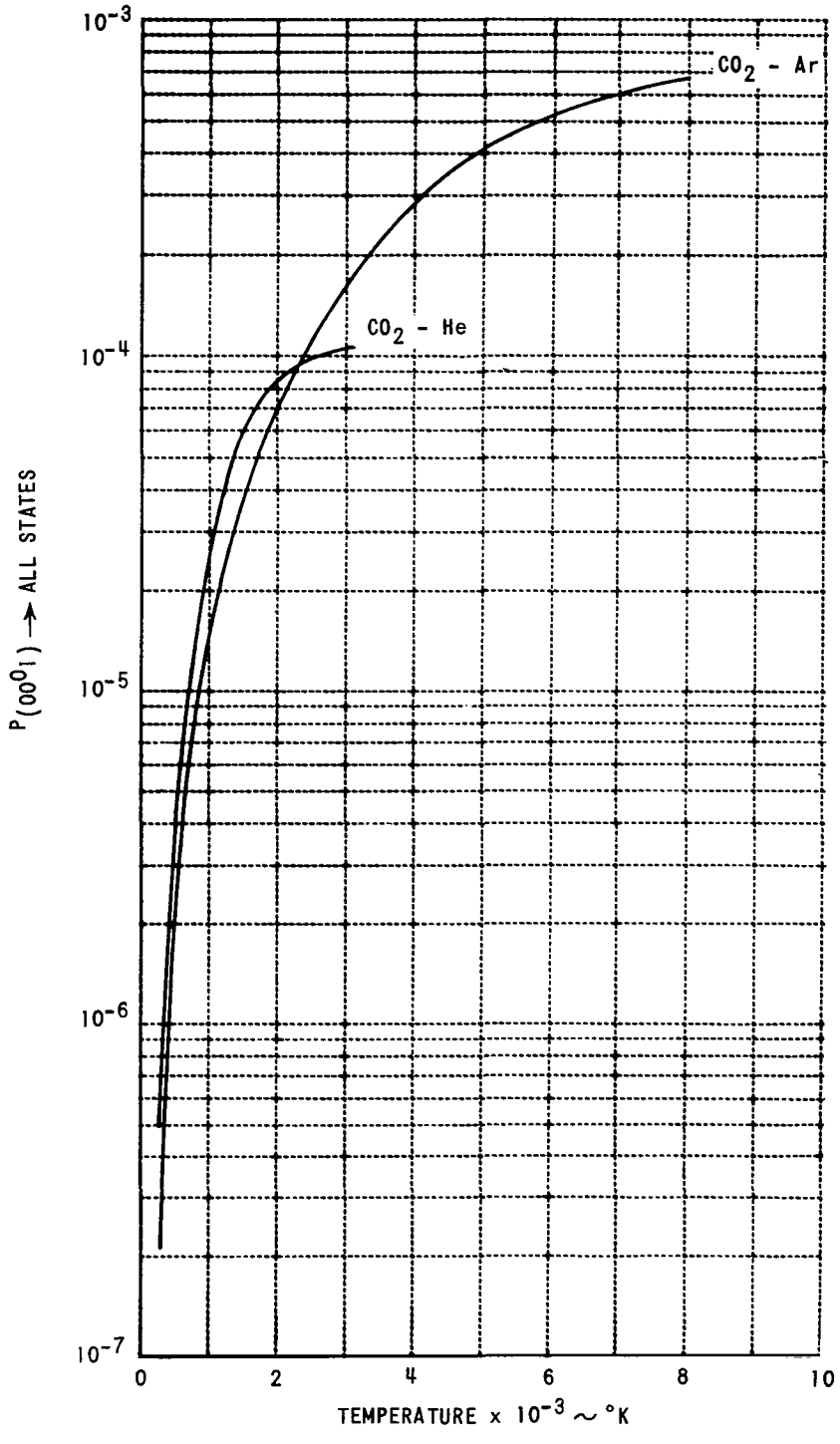

Figure 10 TRANSITIONS FROM (00^01) ASYMMETRIC STRETCHING STATE VS TEMPERATURE.

probability being at the most a factor of two greater than the Ar probability. This behavior contrasts strongly with typical T - V processes (for example, direct deactivation of 00°1 to the ground state), which show very extreme dependence on the mass of the collision partner. This result is in agreement with the experimental data of Yardley and Moore[20] for Ar and He at 300° K. The probabilities given by the present calculation are, however, smaller than those observed at 300° by an order of magnitude.

The extent to which (00°1) is coupled to the other CO_2 states can be assessed by comparing Fig. 10 with Figs. 7 through 9. Examination of these results shows that:

1. The coupling of the ($01^1$0) bending mode state with the (00°1) asymmetric stretch state is much weaker than the ($01^1$0) coupling with the (10°0) symmetric stretch state.

2. In general, relaxation of the (00°1) asymmetric stretch state proceeds much less rapidly than the relaxation of the lower bending and symmetric stretch states ($01^1$0) and (10°0), (02°0), in CO_2-rare gas collisions. (See also Fig. 13.)

These features strongly contribute in creating the powerful cw lasing action at 9.6 and 10.6 in CO_2-He mixtures. Furthermore, relatively weak coupling of the asymmetric stretch to the other CO_2 modes is the justification for the kinetic model of CO_2 laser processes adopted by Moore, et al.[38], by Cool[39], and others. In this model, the bending and symmetric stretching states are assumed to be internal equilibrium, so that a vibrational temperature, T_1, can be assigned to these states. A separate vibrational temperature, T_2, is assigned to the asymmetric stretch states. Such a model appears reasonable for CO_2 strongly diluted by an inert, as in the CO_2 laser. The separation of each of the three modes, and the assignment of separate vibrational temperatures, as done by Basov et al.[40], does not appear useful, in view of the very close ν_1 , ν_2 coupling predicted both by the present analysis as well as by the work of Herzfeld[16] quoted above.

3.4 ENERGY TRANSFER FROM THE (10°0) STATE

In addition to the calculations for energy transfer from the $(01^{1}0)$ and (00°1) states presented in the previous sections, a series of runs was made with the CO_2 molecule initially in vibrational state (10°0).

As in the case of $(01^{1}0)$ deactivation, these probabilities show marked dependence on the initial molecular orientation. Figure 11 shows $P_{(10°0)\rightarrow(02°0)}$ plotted against orientation angle, α_o, again for a coplanar interaction, zero impact parameter, zero initial rotational velocity, and an initial relative velocity of 2×10^5 cm/sec. In contrast to energy transfer from $(01^{1}0)$, both the colinear orientation, $\alpha_o = 0$, and the broadside orientation, $\alpha_o = \frac{\pi}{2}$, are favorable for energy transfer. It must be recalled (see Table 2.1) that both (10°0) and (02°0) are combinations of a stretching and a bending state; energy transfer from these configurations is enhanced by a colinear and a broadside orientation, respectively.

For the $\alpha_o = \frac{\pi}{2}$ initial condition, runs were made over a wide velocity range. The largest of the resulting probabilities are plotted as functions of velocity in Fig. 12. Deactivation of the(10°0)state proceeds almost entirely by transitions to the nearby (02°0), in Fermi resonance with (10°0), and to the nearly uncoupled $(02^{2}0)$. Note that the transition to (02°0) is dominant for velocities $V_o \geq 10^5$; for velocities below this, transition to $(02^{2}0)$ is dominant.

For the purpose of comparison with the calculations of Herzfeld[16] and with available experimental information, these probabilities have been thermally averaged over a Maxwellian velocity distribution, using Eq (3.1), with $\int_o^{\pi/2} d\alpha_o = \frac{\pi}{2}$. The thermally averaged results are shown in Fig. 13. The extremely rapid deactivation of (10°0), even at room temperature, is evident. It is interesting to compare these results with the distorted wave values calculated by Herzfeld. His (10°0) $\longrightarrow$ (02°0) probability, is plotted as the dashed line in Fig. 14. Herzfeld's calculation uses the same repulsive range, ($\alpha_1 = 5 \times 10^8$ cm^{-1}) as the present calculation, but the reduced mass is that for CO_2 - CO_2 collisions ($M = 3.65 \times 10^{-23}$ cm) rather than CO_2 - Ar ($M = 3.47 \times 10^{-23}$ cm). This mass difference is sufficiently slight as to be

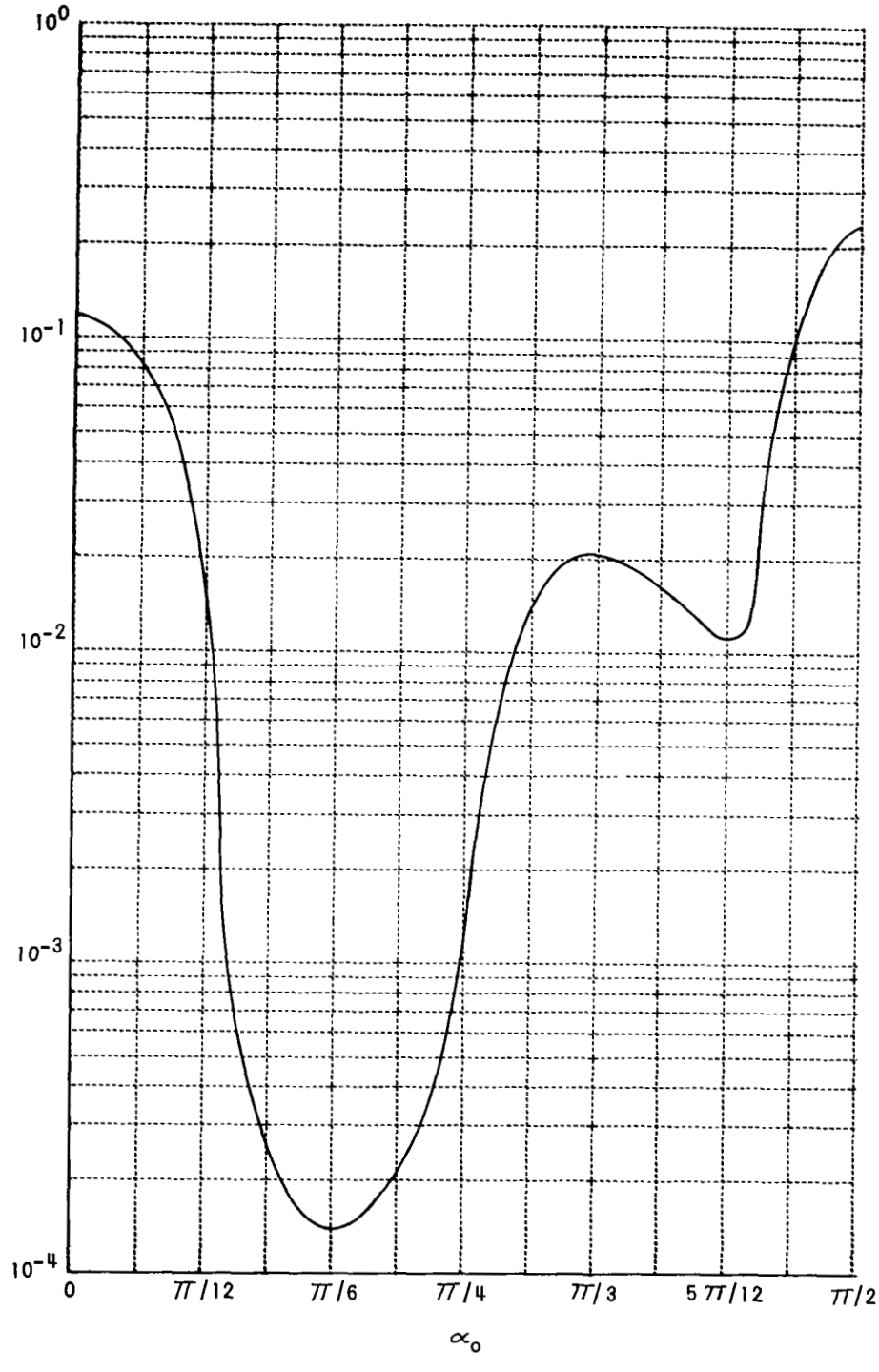

Figure 11 $P_{(10^00)\rightarrow(02^00)}$ TRANSITION VS INITIAL MOLECULAR ORIENTATION. $b = 0$; $V_o = 2 \times 10^5$ cm/sec.

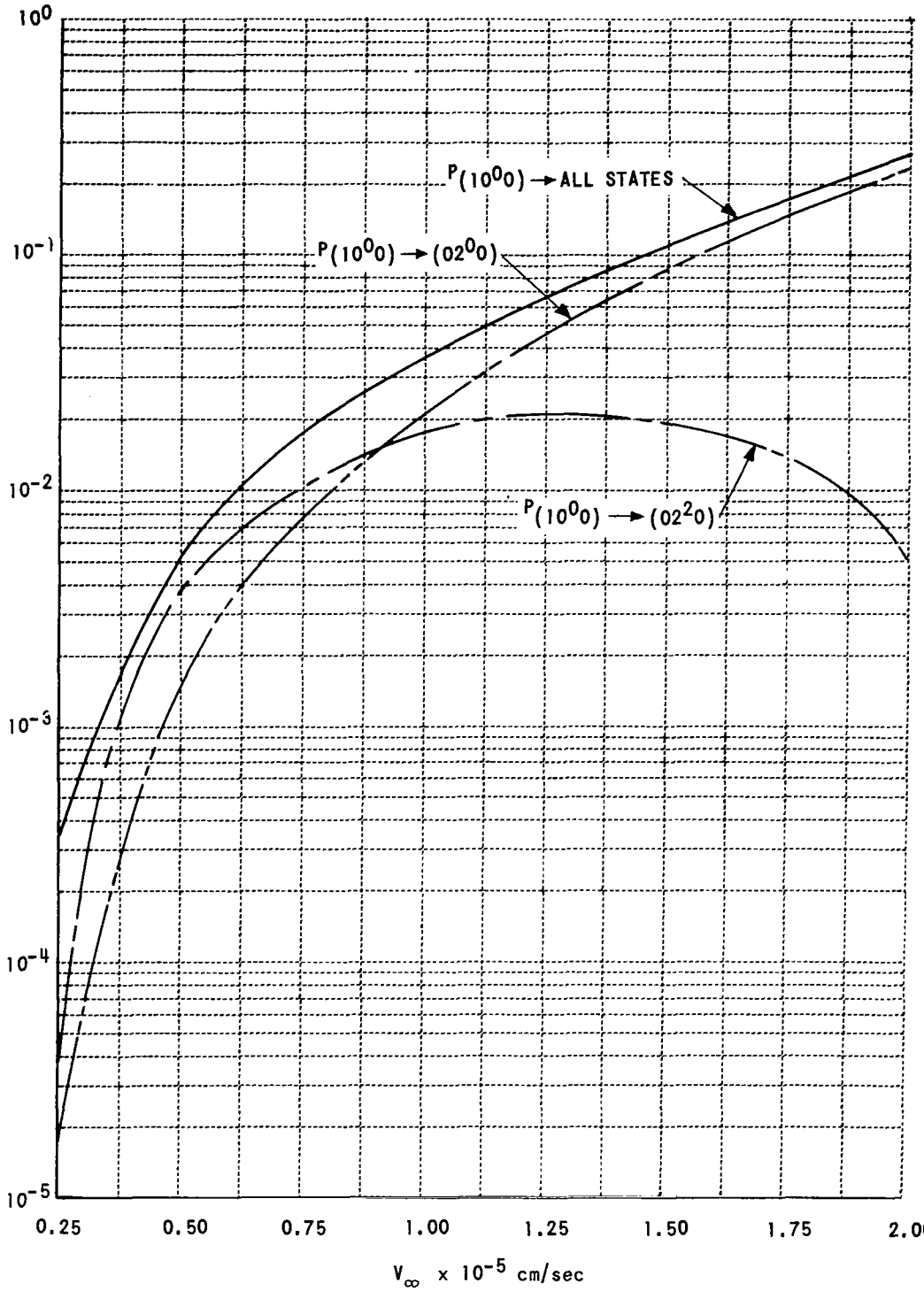

Figure 12 TRANSITIONS FROM (10^00) SYMMETRIC STRETCHING STATE VS VELOCITY.

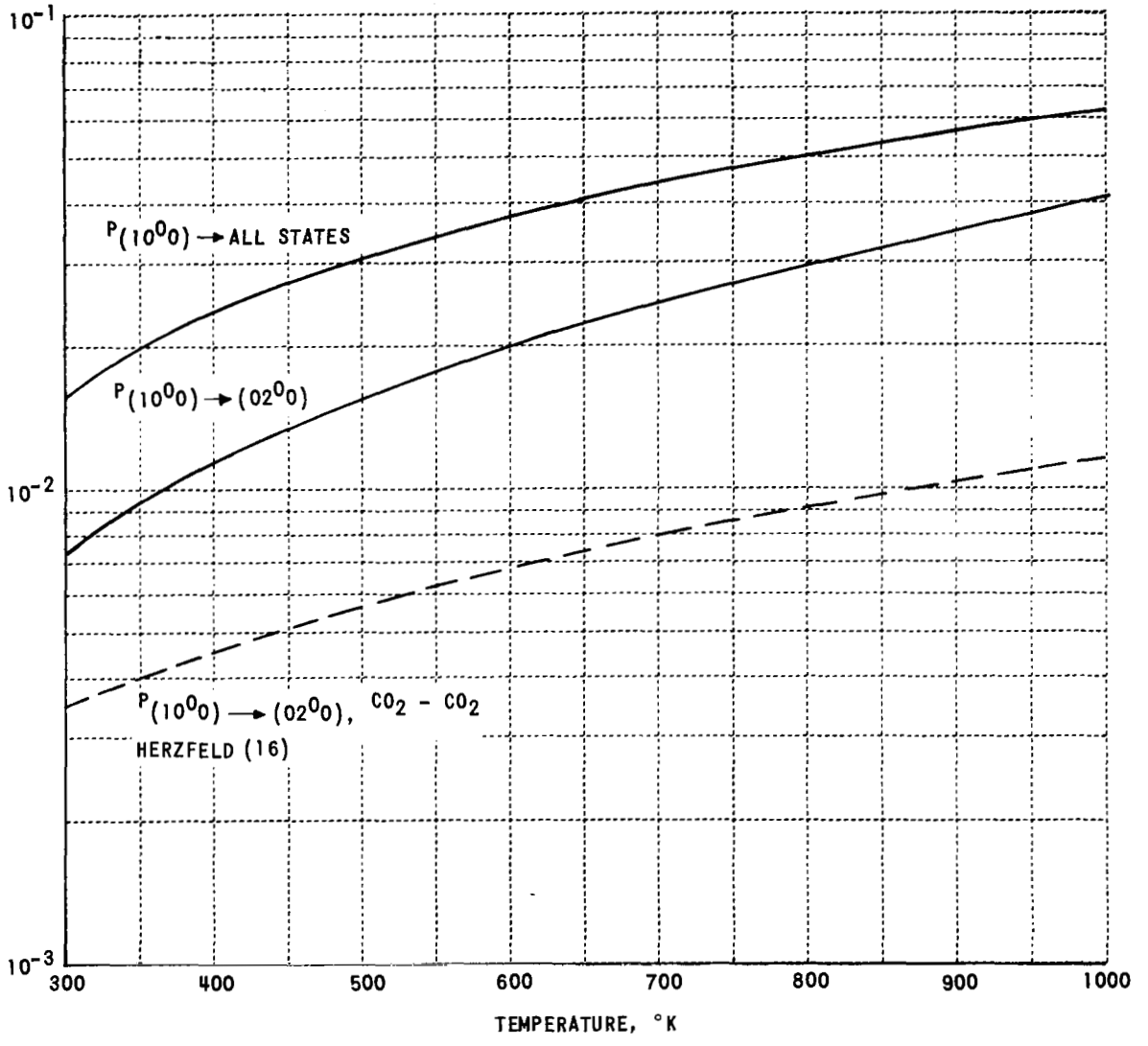

Figure 13 TRANSITIONS FROM (10^00) SYMMETRIC STRETCHING STATE VS TEMPERATURE.

a minor factor in the comparison. The present calculation shows probabilities for this transition 2 - 4 times larger than those of Herzfeld's calculation over the 300°-1000°K temperature range. It should be recalled that the most favorable orientation was chosen for the present estimate of $P_{(10°0)\rightarrow(02°0)}$; results averaged over α_o would be somewhat smaller. The two calculations therefore appear to be in fair agreement.

The only available experimental information on the $(10°0) \longrightarrow (02°0)$ transfer is that provided by Rhodes, Kelley, and Javan,[37] in laser-induced fluorescence studies in pure CO_2. These authors assign a lower limit of 10^6 sec^{-1} $torr^{-1}$ for the rate of this transition, corresponding to a transition probability $P_{(10°0)\rightarrow(02°0)} \cong 8.74 \times 10^{-2}$. This is at least an order of magnitude greater than the CO_2 - Ar probability predicted here. It is likely that at 300° in pure CO_2, long range multipole CO_2 - CO_2 forces control the inelastic processes;[23-25] such interactions are not included in the present model.

Despite the very large $(10°0) \longrightarrow (02°0)$ transition probability, the (10°0) and (02°0) are not directly coupled; the matrix element $\langle 10°0 | V | 02°0 \rangle$ is zero. This aspect of the calculation is similar to the results for (00°1) deactivation given previously in Section 3.3. As discussed in that section, (00°1) deactivation also precedes primarily by transitions to states not directly coupled to (00°1). In the present case, the $(10°0) \longrightarrow (02°0)$ transition occurs primarily through the following two-step processes:

$$CO_2\ (10°0) \longrightarrow CO_2\ (01'0) \longrightarrow CO_2\ (02°0)$$

$$CO_2\ (10°0) \longrightarrow CO_2\ (03'0) \longrightarrow CO_2\ (02°0)$$

$$CO_2\ (10°0) \longrightarrow CO_2\ (11'0) \longrightarrow CO_2\ (02°0)$$

3.5 CONVERGENCE OF A MULTISTATE CALCULATION FOR CO_2

As the discussions in the preceding sections have indicated, the vibrational energy transfer processes in CO_2 often involve the close coupling of several vibrational quantum states, even at moderate collision velocities. As

in the case of calculations for excitation of a simple harmonic oscillator,[36] the number of states which must be included for an accurate calculation of a given transition probability increases with increasing collision energy. However, the nonuniform nature of the energy level separations and coupling matrix elements with increasing energy (c.f. Fig. 3) make a priori prediction of the important states for a given transition and collision energy difficult. The procedure in the calculations of the preceding sections has been to add states until convergence was obtained, any additional added states showing insignificant probability amplitudes throughout the collision trajectory.

In this section, calculations of the $(01^{1}0) \longrightarrow (00^{\circ}0)$ transition, for $b=0$, $\alpha_o = \frac{\pi}{2}$, will be discussed from the viewpoint of the number of states required for convergence.

Figure 14 shows $P_{(00^{\circ}0) \longrightarrow (01^{1}0)}$ calculated at a collision velocity of $V_o = 2 \times 10^5$ cm/sec, plotted against the number of coupled states retained in the calculation, which corresponds to the number of Eq (2.16) retained. The first order perturbation calculation ("PERT," in Fig. 14) is performed by setting $b_{mk} = \delta_{mk}$ on the right hand side of Eq (2.16), where δ_{mk} is the Kronecker delta. This decouples the equations, replacing the sum of the RHS by a single term which may be integrated directly. The first order perturbation approximation assumes that all b_{mk}'s remain very small during the collision except for $k = m$, corresponding to the initial state, which remains ≈ 1, its initial value. The states being added, in addition to the initial $(01^{1}0)$ state itself, are listed in Table 2.1, in the order listed there, i.e., in the order of increasing energy above ground. It was found that states with energies higher than approximately 2000 cm^{-1} did not enter significantly into the calculation of $P_{(00^{\circ}0) \longrightarrow (01^{1}0)}$ at the 2×10^5 cm/sec velocity chosen; as Fig. 14 indicates, convergence was obtained using 8 coupled states.

Figure 14 illustrates the well-known feature[36] that a two-state calculation greatly underestimates the actual value of the transition probability. A second feature of these results, which does not occur in calculations for excitation of diatomiss,

Figure 14 $P_{(01^10)} \rightarrow (00^00)$ TRANSITION PROBABILITY VS NUMBER OF COUPLED STATES.

is that the first order perturbation calculation does not always overestimate the correct value of the probability. In Fig. 14, for example, all calculations using more than four coupled states give a transition probability greater than that calculated using the first order perturbation approximation. This behavior is not observed in a multistate calculation for the transition probability between adjacent states of a simple harmonic oscillator mode.[36] In the case of CO_2, it is a consequence of the fact that states 3, 4, and 5 ((02°0), (10°0), and (02^20), respectively) all lie at approximately the same energy. This threefold degeneracy creates the three possible excitation paths:

$$(00^\circ 0) \longrightarrow (01^1 0) \longrightarrow (x) \longrightarrow (01^1 0) \tag{3.2}$$

where x can be any of the three states mentioned. All these states have energies of approximately twice the $h\nu_2$ energy of the $(00^\circ 0) \longrightarrow (01^1 0)$ fundamental transition being calculated. In a simple harmonic oscillator calculation, there is only one state at this energy level, and hence only one path of the type given in Eq. (3.2).* This effect can be quite common in CO_2, particularly among higher states, where multifold degeneracies occur. Indeed Fig. 14 itself shows a smaller, less dramatic repetition of this effect, as states 6, 7, and 8 are added in the calculation. These states are (03^10), (11^10), and (03^30), respectively. The incremental increase with the addition of each of these states can be observed.

Finally, any truncation of the set (2.16) is an approximation, which will fail at sufficiently high velocities. Figure 15 shows the $(01^10) \longrightarrow (00^\circ 0)$ transition probability, for the same initial orientation as previously discussed, plotted as a function of increasing collision velocity. Figure 16 shows a secondary peak in the transition probability, appearing at higher velocities, which occurs in the 9-state calculation. Such peaks are an artifact of the truncated calculation. The probabilities for the transition between adjacent vibrational states, such as $P_{(00^\circ 0) \longrightarrow (01^1 0)}$, do not actually display such multiple peaks, as a comparison between the ten-state SHO calculation of Sharp and Rapp[36] and the exact results of Treanor[5] indicates. The peaking phenomena of Fig. 15 is quite similar to that observed by Sharp and Rapp, at high velocities in their ten-state calculation for N_2.

---

* The effect is noticeable for this particular transition at quite moderate velocities, the first order perturbation not being accurate at velocities greater than $\sim 5 \times 10^4$ cm/sec.

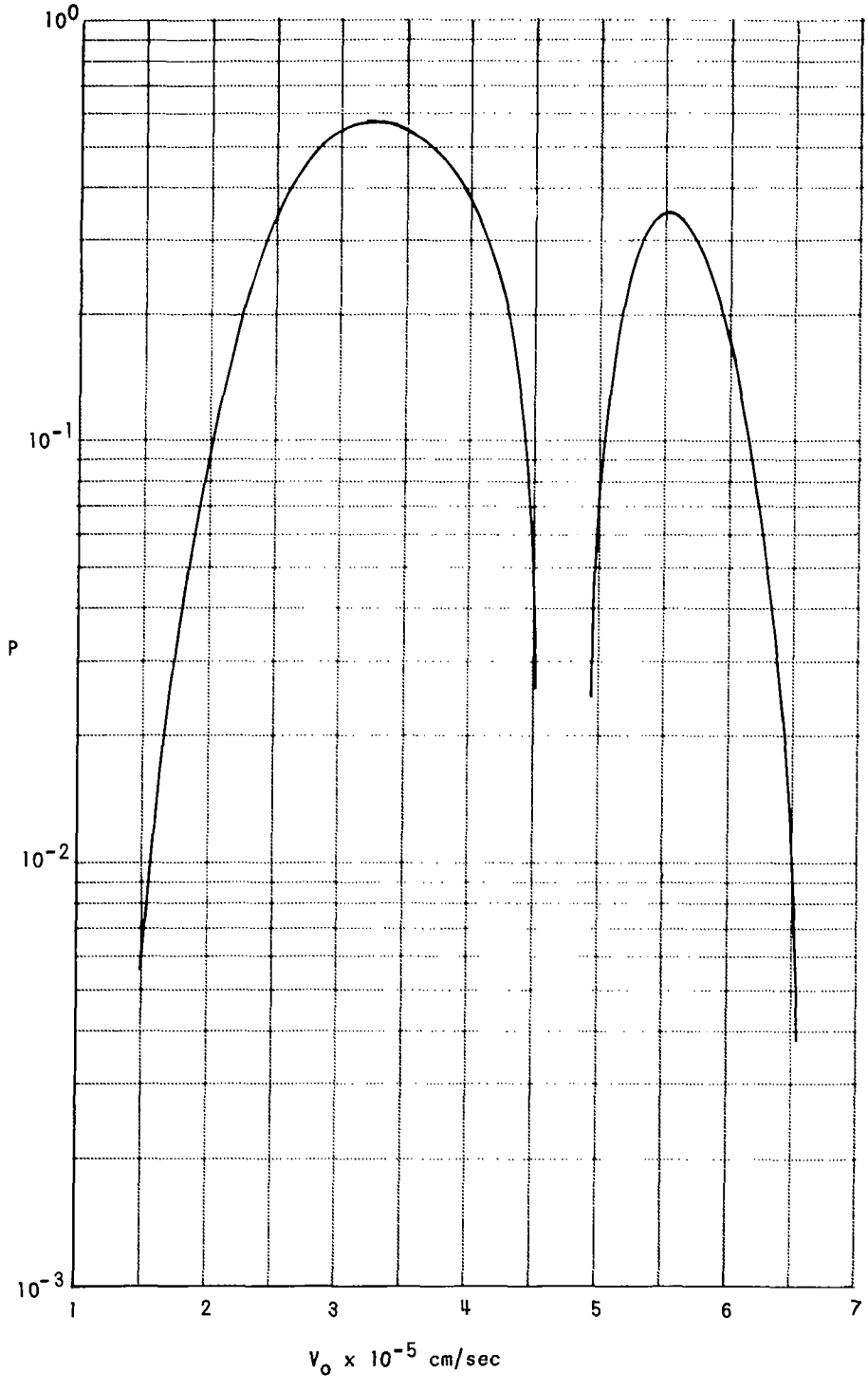

Figure 15 $P_{(01^10) \rightarrow (00^00)}$ TRANSITION PROBABILITY VS VELOCITY FOR BROADSIDE INTERACTION.

4. T-V ENERGY TRANSFER

4.1 DECOUPLED NORMAL MODE MODEL

If certain additional approximations are made in Eq (2.14), its solution may be obtained analytically. Specifically, if in the CO_2 Hamiltonian operator H_v the anharmonicity terms H_2 are neglected, a normal mode description of CO_2 vibration is obtained. If, in addition, only first order terms in the intermolecular potential, V (Eq (2.13)) are retained, it can be shown that Eq (2.14) is separable in the vibrational coordinates. The vibrational excitation process for each mode occurs independently, the modes being completely decoupled. The equations governing the vibrational motion are identical for each mode, and are of the form:*

$$\left[\frac{\hbar^2}{2\mu_i}\frac{\partial^2}{\partial S_i^2} - \frac{1}{2}\mu_i\omega_i^2 S_i^2 + f_i(t)\,S_i\right]\psi_i = i\hbar\,\dot{\psi}_i \,. \qquad (4.1)$$

Here, i denotes the i^{th} vibrational mode of CO_2, and the wave function for the entire system, Ψ, of Eq (2.14) has been factored into the product of the individual mode wave functions, $\Psi = \Pi\,\psi_i$. It is shown in Ref 5 that solution of Eq (4.1) gives the probability P^i_{mn} for transition between the n and m vibrational states of the i^{th} mode to be:

$$P^i_{mn} = m!\,n!\,e^{-\mathcal{E}_i}\,\mathcal{E}_i^{\,m+n}\left[\sum_{j=0}^{\lambda}\frac{(-1)^j\,\mathcal{E}_i^j}{(n-j)!\,j!\,(m-j)!}\right], \qquad (4.2)$$

---

* Some manipulation is necessary to obtain this result for the bending mode coordinates. Putting $S_{2a} = S_2 \sin\gamma$, $S_{2b} = S_2\cos\gamma$, separation is possible; one obtains $\left[\frac{\hbar^2}{2\mu_2}\frac{\partial^2}{\partial S_{2a}^2} - \frac{1}{2}\mu_2\omega_2^2 S_{2a}^2 + f_{2a}(t)\,S_{2a}\right]\psi_{2a} = i\hbar\,\psi_{2b}$, and an identical equation in S_{2b}, f_{2b}, ψ_{2b}, where the forcing functions f_{2a} and f_{2b} are such that $f_{2a}S_{2a} + f_{2b}S_{2b} \equiv f_2 S_2$

where

$$\mathcal{E}_i = \frac{1}{2\mu_i \hbar_i \omega_i} \left| \int_{-\infty}^{\infty} f_i(t)\, e^{i\omega_i t}\, dt \right|^2$$

$$\lambda = \text{lesser of } m, n .$$

Inasmuch as the forcing functions $f_i(t)$ are functions of the collision trajectory parameters (V_o, ρ_o, b_o, α_o, β_o, $\tilde{\gamma}_o$), as discussed in Sections 2.4 - 2.5, Eq (4.2) gives an explicit relation for the T-V transition probability as a function of the trajectory parameters.*

A principal advantage of the decoupled, normal mode calculations described in this section is that they lend themselves to parametric studies of the intermolecular potential functions used in obtaining the basic T-V relaxation rate for CO_2 . The bulk of experimental evidence in pure CO_2 points to rapid equilibration of energy among the CO_2 normal modes, up to high temperatures. Current theoretical examination of intermode energy transfer (Section 3 and Ref 16) supports this rapid equilibration model.** Under such conditions of rapid intermode energy redistribution, the CO_2 T - V relaxation is determined by the bending mode relaxation rate. The present formulation allows the bending mode excitation rate to be calculated independently of the other modes. This simplification permits extensive examination of the influence of potential parameters on the predicted, thermally

---

* The result has already been averaged over the vibrational phase. The ability to do this independently of the trajectory details is a consequence of the decoupling approximation. This same approximation also makes the result independent of the initial vibrational state of the molecule.

** For CO_2 strongly diluted by a vibrational inactive species, such as Ar or He , the ν_3 states are not as closely coupled to the other modes as in the pure gas case. This is due to the absence of rapid intermolecular V-V energy exchange processes such as:

$$CO_2(00^\circ 1) + CO_2(00^\circ 0) \longrightarrow 2\, CO_2(01^\prime 0) ,$$

in the dilute case. However, the ν_1 , ν_2 modes remain closely coupled in the dilute case (c.f. Section 3).

averaged T-V rate, and comparison of these rates with those experimentally measured. Generally, such parametric investigations would be difficult, since each predicted rate is obtained by incorporating many individual trajectory calculations into a thermal averaging scheme. Parametric examination of the resulting rates generally would require a much larger amount of machine time if the influence of all modes has to be incorporated into every trajectory calculation.

A second advantage of the present model is that it permits straightforward calculation of the quantum mechanical transition probability, Eq (4.2). The numerical calculation for the more complex model treated in Section 3 offers much greater difficulty.

The limitations of this model analysis arise from four basic approximations:

1. Semiclassical Approximation
2. Normal Mode Representation of Internal CO_2 Vibrational Motion
3. Linearized Approximation to Intermolecular Potential
4. Decoupling Approximation, i.e., the Neglect of the Influence of Vibration on the Translational-Rotational Motion.

The semiclassical approximation is invoked by treating both the rotational and translational motion of the system classically. The limitations imposed by this common assumption are discussed in standard references.[15] The approximation is unlikely to create any significant limitation for the present application.

The use of a normal mode approximation to the true CO_2 internal energy states does, of course, involve ignoring an important CO_2 feature: the close coupling among states in Fermi resonance. Further, terms coupling the rotational and vibrational motions, created by Coriolis and centrifugal forces, also are neglected. Finally, the normal mode approximation implies small amplitude vibrational bending and stretching. The model given in this section obviously cannot shed any information on intramolecular energy transfer processes. The present analysis, however, is directed toward calculation of the rate for the basic T-V vibrational excitation process. For this purpose, the normal mode approximation can provide useful information.

The last two approximations can be discussed together. Inaccuracies arising from use of the linearized potential and from the decoupling approximation have been assessed in detail for collisions involving diatomics, by Kelley and Wolfsberg,[13] and, recently, by Yao and Yao.[41] Kelley and Wolfsberg have performed exact classical machine calculations for colinear atom-molecule and molecule-molecule collisions, and Yao and Yao have included second-order terms in an analytical solution of the same problem. Their conclusions are in general agreement. These studies indicate that the magnitude of the error due to these approximations depends principally on a parameter involving only the mass of the colliding particles. The error only weakly depends on the potential parameters and collision energy over a wide range of values for these quantities. It is shown[41] that the use of these approximations introduces the largest error when the quantity

$$\tilde{M} = \frac{m_A m_C}{m_B (m_A + m_B + m_C)}$$

becomes large. As mentioned above, these calculations apply to the colinear interaction of an atom and a diatomic harmonic oscillator; m_A and m_B are the masses of the oscillator nuclei, and m_C is the mass of the incident atom. It can be shown that the energy transferred to the vibrational mode, is, in the limit of large collision velocities, given by

$$\Delta E_{V_{MAX}} = 4 \tilde{M} E_o ,$$

where E_o is the initial translational energy of the atom-molecule system. It is seen that for $\tilde{M} > 0.25$, the energy transferred to the vibrational mode will, in the limit of very large collision velocities, exceed the energy available from translation. It is apparent from these relations that, for homopolar molecules, the "worse" cases are light-atom-containing diatomics being struck by very heavy atoms. For a case more similar to CO_2 excitation, we can consider O_2 being struck by Ar. There

$$\tilde{M} = 0.556$$

and

$$\Delta E_{V_{MAX}} = 2.23 E_o$$

For such mass ratios, the calculations of Kelley and Wolfsberg suggest that, over a large range of collisional energies, the ratio of ΔE_v calculated using the decoupling approximation to the exact ΔE_v can be similar to $\Delta E_{v_{MAX}} / E_o$, i.e., in the range 2-3. Thus the decoupling approximation introduces an overestimation of ΔE_v by a factor of 2 to 3.

These error estimates, based on a colinear model for diatomic-atom collisions, cannot be expected to apply exactly to the present case of excitation of CO_2 with a more complex geometry. They are probably a reasonable estimate of the magnitude of error in ΔE_v. A factor of this size in the absolute magnitude of the calculated T-V probabilities cannot be considered critical. Actual high energy failure of energy conservation is predicted in Ref 13 only for extreme collision energies (tens of electron volts). This has been observed in the CO_2 calculation only for ν_2 excitation. Energy conservation failure can be observed in the excitation of the softest (bending) mode, but only when the total energy in translation plus rotation is greater than 20 eV, outside the thermal range of interest in the present study.

4.2 THERMALLY AVERAGED RESULTS

The results presented here are of parametric investigations of the thermally averaged CO_2 transition probabilities.* The calculations were almost entirely for excitation of the CO_2 bending modes, since, due to their low frequency, bending mode excitation is the controlling T-V process in CO_2. Moreover, the calculations require less machine time when confined to the bending modes. Three principal features of the transition probabilities were examined:

1. The effect of potential anisotropy on the thermally averaged probabilities

* A Monte Carlo technique is used to evaluate the thermally averaged probability expression, Eq (2.18). Details of the Monte Carlo method are given in a previous report, CAL No. AM-2438-A-1, and also will be published in the Journal of Computational Physics.

2. The degree of participation of the rotational modes in exciting vibration.
3. The extent of the difference between the coplanar thermally averaged probabilities and the general three-dimensional case.

Figure 16 shows thermally averaged probabilities for coplanar excitation of the bending mode ($\beta_o = \gamma_o = \frac{\pi}{2}$). Probabilities for excitation of the three energy levels, $h\nu_2, 2h\nu_2, 3h\nu_2$ are shown for two values of the potential anisotropy, ℓ = 1.16Å and ℓ = 0.58Å. Note that ℓ = 1.16Å corresponds to the equilibrium C-O internuclear separation in the CO_2 molecule. This value of the anisotropy places the repulsive potential centers at the equilibrium position of the oxygen nuclei. ℓ = 0.58Å corresponds to the repulsive centers being placed at the midpoint of the C-O equilibrium separation. Correlation of calculations[31,42] of rotational relaxation times for homopolar diatomics (using machine computation of coplanar rigid-rotator collisions) with experimental data suggests placement of the repulsive centers at approximately half the equilibrium nuclear separation. For a system as complex as CO_2 - Ar , however, the anisotropy can only be regarded as a potential parameter whose influence must be assessed by calculation. The results of Fig. 16 show marked changes when the anisotropy is varied over the range 1.16Å - 0.58Å. The P_{01} probability is reduced by factors of $\sim$ 1/2 to $\sim$ 1/10, the larger reduction occurring at the lowest temperatures. In addition, the relative influence of the multiple-jump processes is a strong function of the degree of potential anisotropy. In decreasing the anisotropy, the inelastic collision process has been made more adiabatic, decreasing the amount of energy transferred to vibration, and strikingly decreasing the role of multi-jump processes.

Figure 17 shows the degree of participation of the rotational mode in the excitation of bending mode vibration. In computing the "rotation participating" curves, rotational equilibrium has been assumed, and the probabilities are calculated from Eq. (2.18). In computing the "rotation suppressed" curve, the initial rotational energy in each of the trajectories used was set equal to zero. Therefore, in these curves, there is no possibility of any rotational energy input to vibration. It is seen that the rotational contribution can increase P_{01} by factors of $\sim$ 1.5 to 3. The contribution of

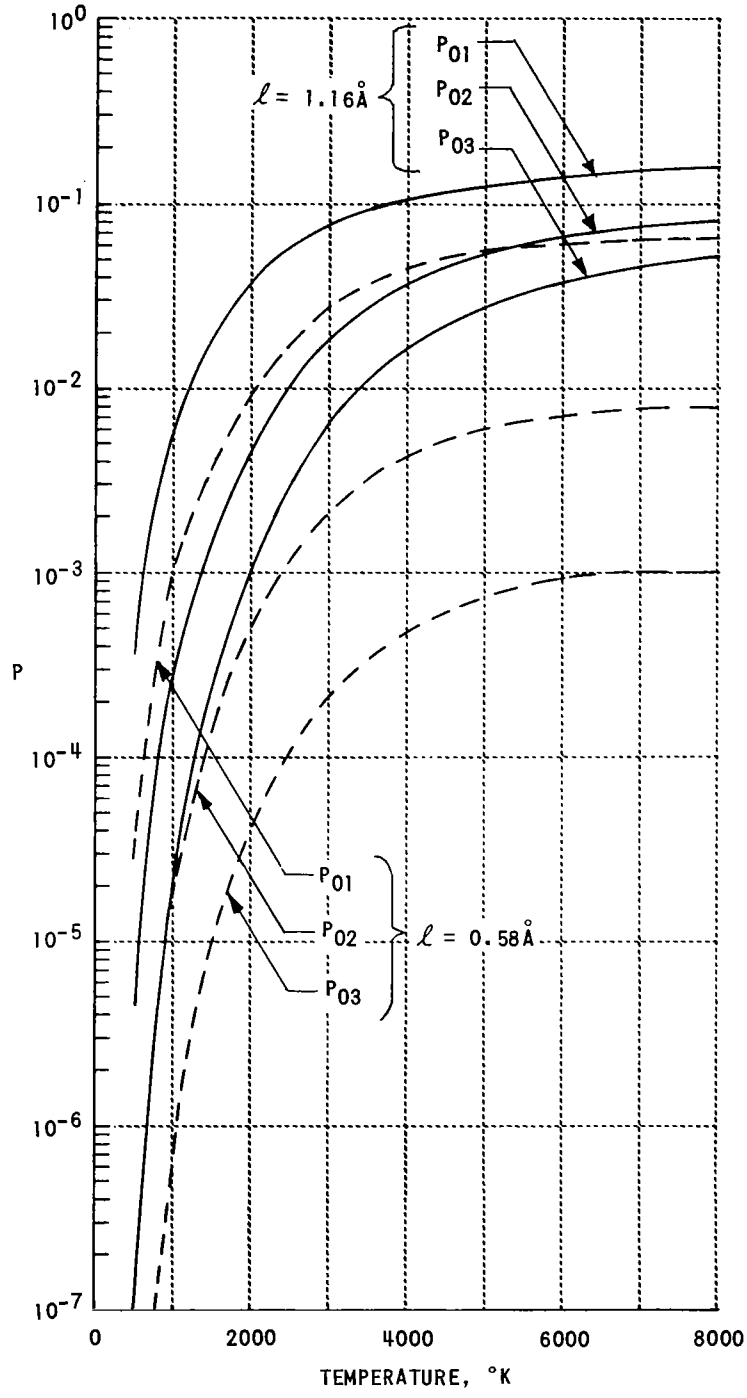

Figure 16 CO_2 BENDING MODE TRANSITION PROBABILITIES VS TEMPERATURE; EFFECT OF POTENTIAL ANISOTROPY.

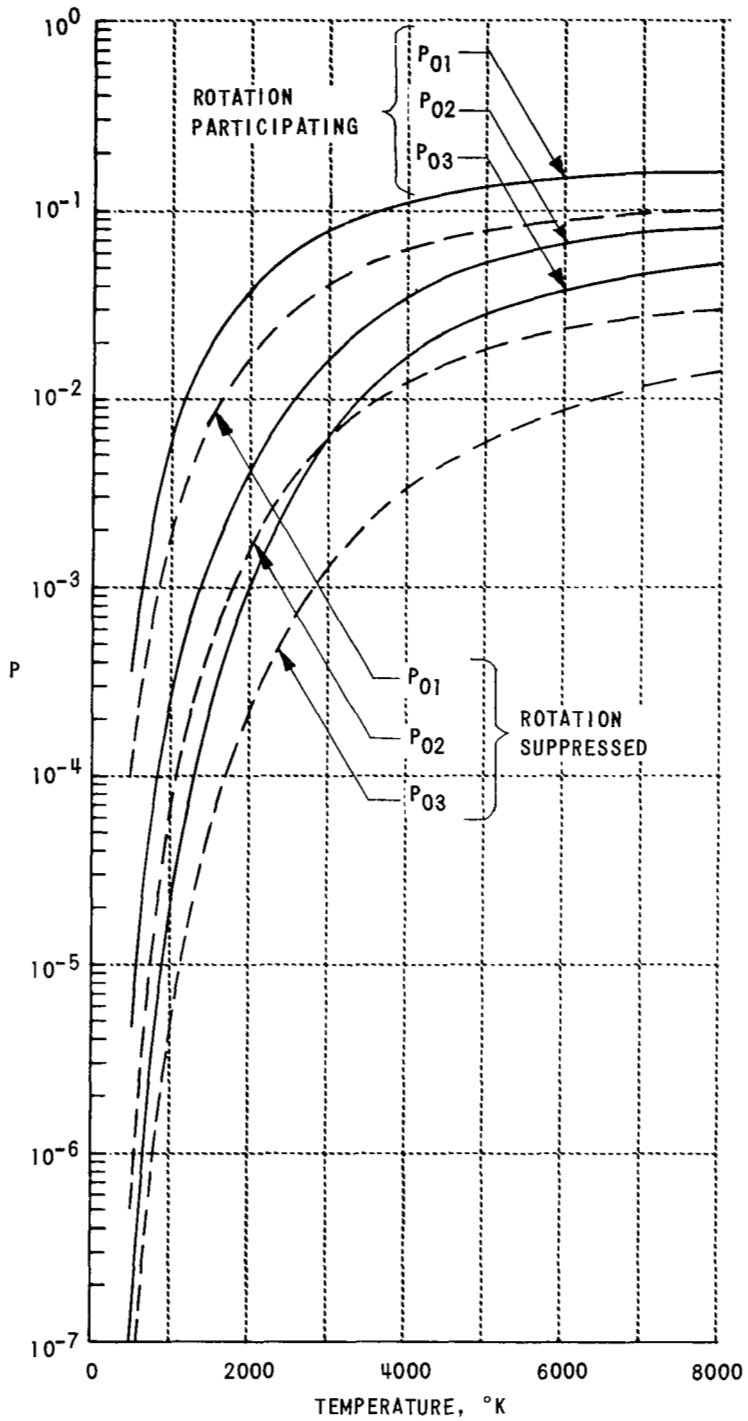

Figure 17 CO_2 BENDING MODE TRANSITION PROBABILITIES VS TEMPERATURE: EFFECT OF MOLECULE ROTATION.

rotation is greatest at the lowest temperatures. Other calculations which include the effect of rotation on vibrational excitation of diatomics have been performed by Benson and Berend[6] and by Kuksenko and Losev.[12] These authors solved, by machine integration, the completely classical equations of motion governing coplanar atom-diatomic molecule collisions. A pairwise additive, nuclei-centered potential similar to Eq (2.2) was used. In both cases, molecular constants for O_2 - Ar collisions were used. Kuksenko and Losev[12] discuss the effect of rotation on the thermally averaged energy transferred to vibration, $\overline{\Delta E}_v(T)$. They find rotation increases $\overline{\Delta E}_v$ by "4 to 5" at 1000°K, but above 1500°, the increase due to rotation is only "a few percent." The quantity $\overline{\Delta E}_v$ is only directly equivalent to $P_{o,1}(T)$ in the limit of low collision energies, as discussed in Ref 5. For this reason, and also because of the difference in potential parameters and molecular masses, detailed comparison of the two calculations is not possible. The general magnitude of the rotational effect in the present result at the lower temperatures, however, seems to be consistent with those observed in Ref 12. The contribution of rotation is seen to be greater in multi-jump probabilities (Fig. 17). All the results shown are for $\ell = 1.16\text{Å}$; the rotational contribution, of course, becomes less with decreasing potential anisotropy.

A general, three-dimensional calculation of the bending mode excitation probabilities is shown in Fig. 18. The potential anisotropy is $\ell = 1.16\text{Å}$, and all other parameters are the same as those of the coplanar results shown in Fig. 16. Comparison with the $\ell = 1.16\text{Å}$ curves of Fig. 16 shows very slight difference between the three dimensional and coplanar results. It should be noted that, in the normal mode model of the CO_2 vibrational states used for the calculations of this section, allowance must be made for the degeneracy of the bending mode in the general, three-dimensional case. It can be shown that the total probability for excitation from ground to states with energy $n h\nu_2$ is:

$$P_{on} = \sum_{ALL\ j+k=n} P_{oj}^{(a)} P_{ok}^{(b)}, \qquad (4.3)$$

where $P_{oj}^{(a)}$ and $P_{ok}^{(b)}$ are the probabilities for the separate excitation of the

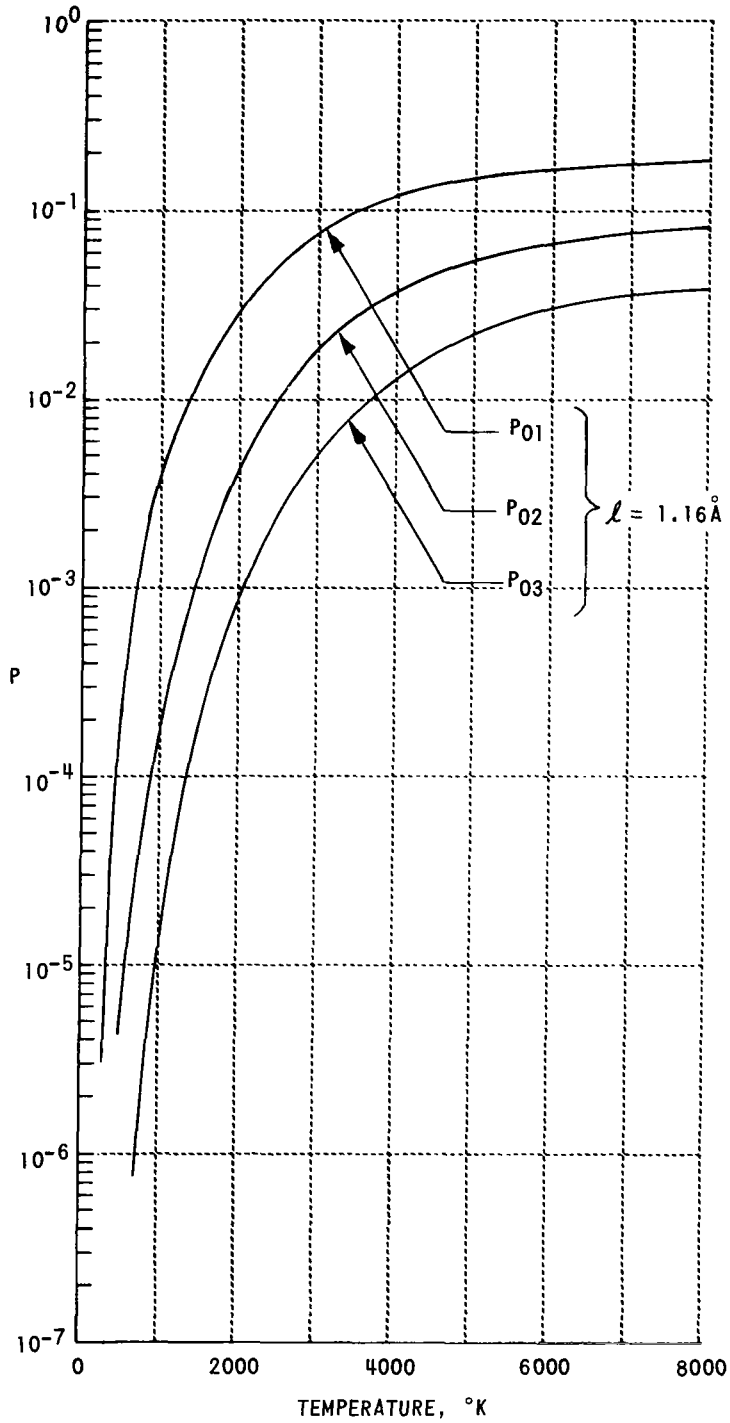

Figure 18 CO_2 BENDING MODE TRANSITION POSSIBILITIES VS TEMPERATURE; THREE-DIMENSIONAL CALCULATION

orthogonal, degenerate bending modes a and b. The three-dimensional results of Fig. 18 have been obtained using Eq (4.3).*

Finally, Fig. 19 shows a comparison of the present calculation (for two values of potential anisotropy) with the distorted wave calculation of Herzfeld[16] and the best fit to a large amount of experimental data, as compiled by Taylor and Bitterman,[26] for bending mode excitation in CO_2 - CO_2 collisions. It is seen that the probabilities predicted by the Herzfeld theory fall between the values given in the present calculation for $\ell = 1.16\text{Å}$ and $\ell = 0.58\text{Å}$.** Both calculations exhibit a similar temperature dependence, which is quite close to the Landau-Teller[44] dependence of $\ln P_{o1} \propto T^{-1/3}$. The fit to the experimental data shows a somewhat flatter temperature dependence. Furthermore, the experimental results fall as much as a factor of three below the calculated values for 0.58Å — 1.16Å, in the middle of the temperature range. For an extended discussion of the sources of the data used to obtain the experimental curve in Fig. 19, reference should be made to the survey of Taylor and Bitterman.[26]

The CO_2 molecule is one of the few species for which experimental data are available over such a large temperature range, 6000°K being more than six times the characteristic temperature of the bending mode, $\theta_{\nu_2} = 960°\text{K}$. It must be emphasized, however, that neither the experimental data nor the calculations are such that precise quantitative comparisons can be expected. There is more than an order of magnitude variation among the reported data

---

* Both coplanar and three-dimensional probabilities have been thermally averaged using Eq (2.18), i.e., a three-dimensional Maxwellian distribution. For coplanar cases, the angles β and γ are such that $\beta = \pi/2$ and $\gamma = \pm \pi/2$ throughout the collision, and Eq (2.18) reduces to an integral over four variables.

** Herzfeld's calculation uses an exponential repulsive potential acting between the nuclei of the colliding molecules. It is not, however, a general three-dimensional calculation, but employs a rather sophisticated estimate of steric effects. Direct comparison of geometrical effects in the two calculations does not seem possible.

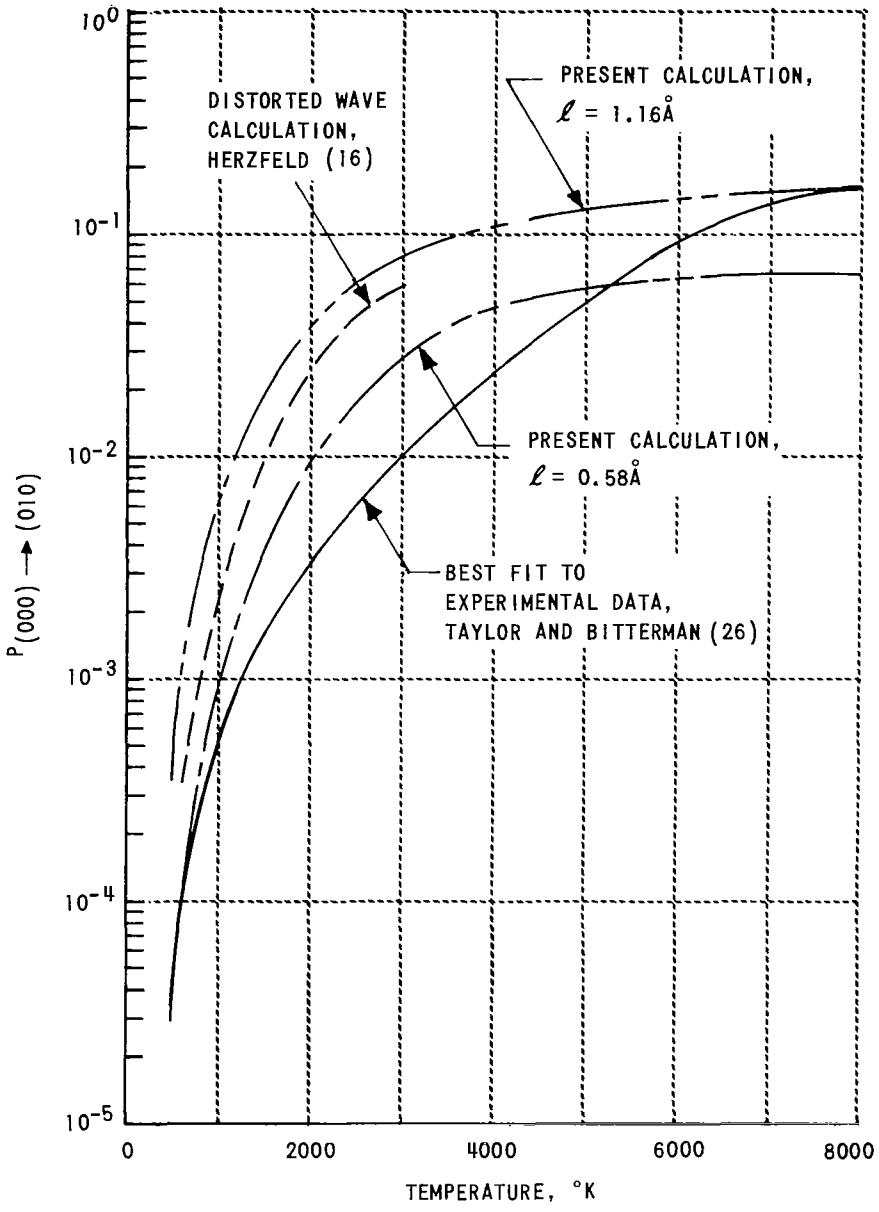

Figure 19 CO_2 BENDING MODE EXCITATION, $P_{(000)\rightarrow(010)}$. COMPARISON OF THEORETICAL AND EXPERIMENTAL DATA ON CO_2 - CO_2 COLLISIONS.

of the various experiments used to obtain the curve of Fig. 20 at lower temperatures.* And, as has already been discussed, the semiempirical nature of the potential function chosen introduces large uncertainties in theoretical calculation of the rate of CO_2 vibrational excitation. Given these uncertainties in both the theoretical calculations and the experimental data, the degree of correlation shown in Fig. 20 is satisfactory.

---

* Above 1500°K, the experimental curve is the mean of the data of the one shock tube experiment of Camac.[45] Below this temperature, the curve represents more than a score of separate experiments (c.f. Ref 26).

5. SUMMARY

This report has presented the formulation and analyses of models which allow calculation of cross sections for the vibrational excitation of CO_2 during molecular collisions. The basic processes modeled are energy transfer between CO_2 vibrational states (intramolecular V-V processes), and energy transfer from the translational and rotational modes of the gas into the vibrational modes of the CO_2 molecule (T-V processes). Emphasis is placed on calculating trajectories and energy transfer for the inelastic collision of a structureless (i.e., nonvibrating, spherically symmetric) particle with a CO_2 molecule.

Previous analyses of inelastic collisions of a CO_2 molecule with a second particle have suffered from at least one of the following restrictions: (1) The calculation of the inelastic cross section has been restricted to that of first-order perturbation theory. (2) The nonspherical nature of the potential has been neglected. (3) The effect of rotation of the CO_2 molecule on the energy transfer has been neglected. (4) The influence of vibrational bending of the CO_2 molecule on the energy transfer has been neglected. (5) Intermode coupling during the collision has been ignored. The present studies have been directed toward including these features of the collision in the analysis. The details of the present model are given in Section 2 of this report.

Modelling and analysis of the collision-induced intramolecular (V-V) processes among the coupled vibrational modes of CO_2 is presented in Section 3. A multistate, semiclassical treatment is used, with allowance for anharmonic coupling of the vibrational modes. Results of detailed calculations are presented for energy transfer from the $(01^{1}0)$, $(00^{\circ}1)$, and $(10^{\circ}0)$ states of CO_2. These calculations display the extremely close coupling between the bending and symmetric stretch modes. Excitation of the $(10^{\circ}0)$ state proceeds via transitions from $(01^{1}0)$, not directly from the ground $(00^{\circ}0)$ state. The asymmetric stretching mode is much less closely coupled to the bending mode in rare gas collisions, lending support to the "two temperature" kinetic modelling of the CO_2 vibrational modes.[38,39] Relaxation

of the (00°1) asymmetric stretch state occurs principally to the (ν_1, ν_2) Fermi resonance states; deactivation by transitions to the (00°0) ground state or the ($01^1$0) bending state is negligible. The (00°1) relaxation has only slight mass dependence, as shown by comparison of calculations for CO_2 - Ar and CO_2 - He collisions. This result agrees with the experimental data of Yardley and Moore,[20] although, for the particular potential constants used in this calculation, the values of the (00°1) deactivation rates at 300° are approximately an order of magnitude less than those observed.

An important feature of the present multistate calculation is that, in the case of (00°1) and (10°0) relaxation, energy transfer primarily occurs to levels not directly coupled to these initial states. Deactivation takes place by transitions through an intermediate state or states. Such processes, which appear to be dominant in intramolecular CO_2 vibrational relaxation, cannot be calculated on the basis of a first order perturbation approximation.

All the transition probabilities calculated with the coupled-mode model showed marked dependence on initial molecular orientation.

Finally, general features of a multistate calculation, and differences between a multistate calculation and a first order perturbation calculation of CO_2 vibrational excitation were examined. In contrast to vibrational excitation of a single harmonic oscillator, it was found that, under certain collision conditions, the multistate calculation could give a larger transition probability than a first order perturbation calculation, due to near-coincidence of more than one CO_2 energy level.

Modelling and analysis of the T-V energy transfer process is treated in Section 4. The decoupled-normal-mode (DNM) model presented in these sections retains such features as a nonspherically symmetric intermolecular potential, the influence of molecular rotation, and the influence of the vibrational bending modes. The inclusion of these features is desirable for the specific case of CO_2 T-V excitation, wherein the role of the bending modes is expected to be significant.

As discussed in Section 1, any cross section calculation for the vibrational excitation of CO_2 currently must rely on empirically derived potential

data. It is therefore desirable that a model calculation of thermal T-V cross sections be sufficiently flexible to allow investigation of the effects of various collision parameters, without requiring an impractical amount of machine computation time. The DNM model permits computation of the vibrational transition probabilities in such a sufficiently short time. This reduction in the computational time is achieved in three ways. First, the decoupling approximation reduces the number of initial trajectory parameters involved; in particular, the need for averaging over the various vibrational phases and energies is eliminated. Thus the dimensionality of the thermal cross-section integral (Eq (3.1)) has been significantly reduced. A second feature of the DNM model is that T-V excitation of the various CO_2 modes can be examined independently. In particular, if the bending mode excitation is the basic T-V mechanism, then the T-V excitation of this mode can be calculated separately. A much larger amount of machine time would be required if the influence of all vibrational modes had to be incorporated into every trajectory calculation. Finally, the Monte Carlo thermal averaging scheme used greatly reduces the number of trajectory calculations required over more conventional numberical quadrature techniques.

Using the decoupled normal mode model, three principal features of the CO_2 T-V transition probabilities were examined:

1. The effect of potential anisotropy on the thermally averaged probabilities.
2. The degree of participation of the rotational mode in exciting vibration.
3. The extent of the difference between the coplanar thermally averaged probabilities and the general three-dimensional case.

It was found that the degree of potential anisotropy has a large effect on the magnitude of the CO_2 T-V transition probabilities. When the anisotropy is varied between physically reasonable limits, the excitation probability changes by factors of 2-10, the greatest change occurring at the lower temperatures. In addition, the relative influence of the multiple-jump processes is a strong function of the degree of potential anisotropy.

Rotational energy was found to contribute to vibrational excitation of

CO_2 , increasing the magnitude of bending state excitation by as much as a factor of 3 at the lowest temperatures (= 300°K). The magnitude and nature of the rotational contribution seen in this study appears to be in general agreement with the results of Kuksenko and Losev.[12]

The three-dimensional calculation for CO_2 bending mode excitation did not differ significantly from the coplanar case, over the entire temperature range studied (300 - 8000°K).

The current calculation of bending mode excitation probabilities bracketed the theoretical results of Herzfeld, when the potential anisotropy was varied between 1.16Å and 0.58Å. The theoretically predicted transition probabilities for a potential anisotropy of 0.58Å were within a factor of three of the mean of experimentally measured values, over the temperature range 300 to 8000°K. The T-V model therefore appears quite adequate for the correlation of high temperature shock wave data.

REFERENCES

1. Rapp, D. and Kassal, T., "A Review of the Theory of Vibrational Energy Transfer Between Simple Molecules in Nonreactive Collisions," Grumman Research Dept., Rept. RE-345, Grumman Aircraft Engineering Corp., Bethpage, New York, Oct. 1968; also Chem. Rev. 69, 61 (1969).

2. Rich, J. W. and Treanor, C. E., "Vibrational Relaxation in Gas Dynamic Flows," Ann. Rev. of Fluid Mechanics, W. G. Vincenti, Ed., Annual Reviews, Palo Alto, to be published (1970).

3. Borrell, P., Advances in Molecular Relaxation Processes, I, 69 (1967).

4. Burnett, G. M. and North, A. M., Eds., Transfer and Storage of Energy of Molecules. Vol. 2. Vibrational Energy. Wiley-Interscience, London (1969).

5. Treanor, C. E., J. Chem. Phys. 43, 532 (1965).

6. Benson, S. W. and Berend, G. C., J. Chem. Phys. 44, 4247 (1966).

7. Sharp, T. E. and Rapp, D., J. Chem. Phys. 43, 1233 (1965).

8. Mies, F. H., J. Chem. Phys. 42, 2709 (1965).

9. Takayanagi, K., Progr. Theoret. Phys. (Kyoto) Suppl. No. 25, 1 (1963).

10. Takayanagi, K., Adv. in Atomic and Molecular Phys. 1, 149 (1965).

11. Kuksenko, B. V., et al., Dokl. Akad. Nauk SSSR 167, 6, 1280 (1966).

12. Kuksenko, B. V. and Losev, S. A., Dokl. Akad. Nauk SSSR 178, 6 (1968). Sov. Phys. - Dokl., 13, 142 (1968).

13. Kelley, J. D. and Wolfsberg, M., J. Chem. Phys. 44, 324 (1966).

14. Secrest, D. and Johnson, B. R., J. Chem. Phys. 45, 4556 (1966).

15. Mott, N. F. and Massey, H. S., The Theory of Atomic Collisions, 3rd Ed., Oxford Univ. Press (1965).

16. Herzfeld, K. F., J. Chem. Phys. 47, 743 (1967).

17. Marriott, R., Proc. Phys. Soc. 88, 83 (1966).

18. Witteman, W. J., J. Chem. Phys. 35, 1 (1961).

19. Shields, F. D. and Burks, J. A., J. Acoust. Soc. Am. 43, 510 (1968).

20. Yardley, J. T. and Moore, C. B., J. Chem. Phys. 46, 4491 (1967).

21. Shin, H. K., Chem. Phys. Letters 2, 629 (1968).

22. Grimaldi, J. J., Endres, P. F. and Wilson, D. J., J. Chem. Phys. 50, 1627 (1969).

23. Sharma, R. D. and Brau, C. A., Phys. Rev. Letters 19, 1273 (1967).

24. Sharma, R. D. and Brau, C. A., J. Chem. Phys. 50, 924 (1969).

25. Sharma, R. D., J. Chem. Phys. 50, 919 (1969).

26. Taylor, R. L. and Bitterman, S., "Survey of Vibrational Relaxation Data for Processes Important in the CO_2 - N_2 Laser System," Rev. Mod. Phys. 41, 26 (1969). Also AVCO Everett Research Labs. Report No. 282 (October 1967).

27. Karplus, M. and Raff, L. M., J. Chem. Phys. 41, 1267 (1964).

28. Raff, L. M., J. Chem. Phys. 44, 1202 (1966).

29. Houghton, J. T., Proc. Phys. Soc. 91, 439 (1967).

30. Parker, J. G., Phys. Fluids 2, 449 (1959).

31. Raff, L. M., J. Chem. Phys. 46, 520 (1967).

32. Herzberg, G., Molecular Spectra and Molecular Structure II, Infrared and Raman Spectra of Polyatomic Molecules, D. Van Nostrand Co., Inc., Princeton (1945).

33. Dennison, D. M., Phys. Rev. 41, 304 (1932).

34. Adel, A. and Dennison, D. M., Phys. Rev. 43, 716; 44, 99 (1933).

35. Rapp, D. and Sharp, T. E., J. Chem. Phys. 38, 2641 (1963).

36. Sharp, T. E. and Rapp, D., J. Chem. Phys. 43, 532 (1965).

37. Rhodes, C., Kelley, M. and Javan, A., Bull. Am. Phys. Soc. 13, 597 (1968).

38. Moore, C. B., Wood, R. E., Hu, B. L. and Yardley, J. T., J. Chem. Phys. 46, 4222 (1967).

39. Cool, T. A., J. Appl. Phys. 40, 3563 (1969).

40. Basov, N. G., Mikhailov, V. G., Oraeyskii, A. N. and Shcheglov, V. A., Z. Tek. Fiz. 38, 2031 (1968); Sov. Phys.-Tech. Phys. 13, 1630 (1969).

41. Yao, H. Y. and Yao, S. J., J. Chem. Phys. 51, 296 (1969).

42. Lordi, J. A. and Mates, R. E., Phys. Fluids 13, 291 (1970).

43. Cottrell, T. L. and McCoubrey, J. C., Molecular Energy Transfer in Gases, Butterworths, London (1961).

44. Herzfeld, K. F. and Lito Vitz, T. A., Absorption and Dispersion of Ultrasonic Waves, Academic Press, New York (1959).

45. Camac, M., in Fundamental Phenomena in Hypersonic Flows, (J. G. Hall), Ed.), p. 195, Cornell Univ. Press (1966). Also, AVCO Everett Research Lab. Report No. 194 (1964).

NASA-Langley, 1971 —— 24